Phospholipid Flippase Activity and Cellular Function of Class 5 P4-ATPases

2016

Tomoki Naito

TABLE OF CONTENTS

GENERAL INTRODUCTION

Cellular membranes have multiple functions, which are conferred by the unique composition and organization of proteins and lipids. In eukaryotic cells, lipid bilayers of the plasma membrane and organelle membranes exhibit asymmetric distribution of phospholipids (1-3). For example, in human erythrocytes, phosphatidylserine (PS) and phosphatidylethanolamine (PE) are restricted primarily to the inner leaflet of the plasma membrane, whereas phosphatidylcholine (PC) and sphingomyelin (SM) are enriched on the cell surface (Fig. 0-1) (4, 5). Regulated exposure of PS to the outer leaflet is critical for some biological processes, such as apoptotic cell death, platelet coagulation, and fusion of muscle cells (5-7), indicating the importance of lipid asymmetry at steady state. The asymmetric distribution of phospholipids is maintained and regulated by energy-dependent transbilayer lipid translocases, flippases and floppases. It is defined that "flip" indicates a unidirectional translocation of phospholipids from the exoplasmic/luminal to the cytoplasmic leaflet in biological membranes and "flop" indicates a translocation in the opposite direction.

An ATP-dependent aminophospholipid translocase activity was discovered in the plasma membrane of human erythrocytes (8). Subsequently, type IV P-type ATPases (P4-ATPases), which is a subfamily of P-type ATPase superfamily, were identified as flippases in eukaryotic cells (Fig. 0-1) (9-13). In general, P-type ATPases transport cations across membranes (e.g. H^+/K^+-ATPase, Na^+/K^+-ATPase, Ca^{2+}-ATPase, *etc.*), whereas P4-ATPases translocate phospholipids, which are much larger than cations (Fig. 0-2). P4-ATPases are present in all eukaryotic cells and current knowledge on cellular functions of P4-ATPases is mostly derived from studies in the yeast *Saccharomyces cerevisiae* (Fig. 0-3). Like other P-type ATPases, flippase activities of P4-ATPases are coupled to their ATPase cycle, called Post-Albert cycle (Fig. 0-2) (14). Mammals express 14 P4-ATPases: class 1 (ATP8A1, ATP8A2, ATP8B1, ATP8B2, ATP8B3, and ATP8B4), class 2 (ATP9A and ATP9B), class 5 (ATP10A, ATP10B, and ATP10D), and class 6 (ATP11A, ATP11B, and ATP11C) (Fig. 0-3). In contrast, yeast contains five P4-ATPases (Drs2p, Neo1p, Dnf1p, Dnf2p, and Dnf3p) (Fig. 0-3). P4-ATPases form a heteromeric complex with members of the CDC50 family (CDC50A, CDC50B, and CDC50C) (Fig. 0-3) (12, 15). CDC50 proteins are believed to

be a chaperone-like protein for P4-ATPases and most mammalian P4-ATPases, except for ATP9A and ATP9B, require association with CDC50 proteins for their exit from the endoplasmic reticulum (ER) and subsequent subcellular localization (Fig. 0-3) (16-20).

Historically, aminophospholipid translocase activity was first found in erythrocytes and the responsible protein was identified as ATP8A1 (a member of P4-ATPase family, Fig. 0-3). Thus, P4-ATPases were thought to flip aminophospholipids, although it has been reported that even PC can be translocated by yeast P4-ATPases (11). In the previous study, our laboratory showed that ATP11A and ATP11C flip NBD-labeled aminophospholipids, NBD-PS and -PE, and ATP8B1 and ATP8B2 preferentially flip NBD-PC at the plasma membrane (21).

The phospholipid asymmetry regulated by P4-ATPases is indispensable for homeostasis of multicellular organisms. Loss of phospholipid asymmetry due to mutations in the human FIC1/ATP8B1 gene causes progressive familial intrahepatic cholestasis 1 (PFIC1) (22, 23). Our laboratory previously showed that some of ATP8B1 mutants found in PFIC1 patients failed to flip PC, indicating that PC flipping activity at the bile canaliculi is critical for proper bile excretion in liver (21). Mutations in ATP8A2 are associated with a severe neurological disorder characterized by cerebellar ataxia, mental retardation, and disequilibrium syndrome (24). ATP11C deficiency causes a defect in B-cell maturation, altered erythrocyte shape, and anemia (25, 26). During apoptosis, ATP11C undergoes caspase-mediated cleavage and is consequently inactivated, resulting in PS exposure on the cell surface (27). Heterozygous deletion of ATP10A in mice causes diet-induced obesity, type 2 diabetes, and nonalcoholic fatty liver disease, implicating ATP10A in obesity-related metabolic abnormalities (28). ATP10A is also implicated in regulation of insulin-stimulated glucose uptake (29, 30). *ATP10D* variants are associated with myocardial infarction in German population and with atherosclerosis in Japanese elderly population (31, 32). However, the enzymatic characteristics, subcellular localization, and cellular functions of class 5 P4-ATPases (ATP10A, ATP10B, and ATP10D) remain unknown.

In this study, I first characterized the interaction of class 5 P4-ATPases with CDC50 proteins and determined their subcellular localization (Chapter 1). Next, I investigated their flippase activities and found that ATP10A exhibited a flippase activity toward NBD-PC but not toward NBD-aminophospholipids. Moreover, I found that

enhanced PC flipping activity in cells due to exogenous ATP10A expression caused a change in cell morphology and dynamic state of β1-integrin resulting in delayed cell adhesion and cell spreading (Chapter 2).

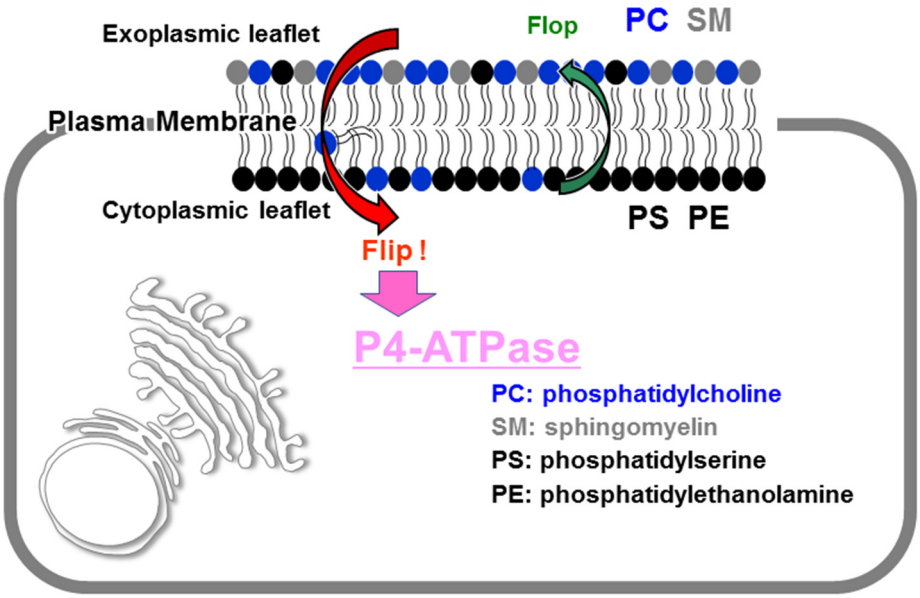

Fig.0-1. Establishment and maintenance of phospholipid asymmetry in the plasma membrane.

In eukaryotic cells, the distribution of phospholipids is different between the exoplasmic and cytoplasmic leaflet. In the plasma membrane, PS and PE are concentrated in the cytoplasmic leaflet, whereas PC and SM are enriched in the exoplasmic leaflet. This asymmetric distribution of phospholipids is maintained and regulated by transbilayer phospholipid translocation, called “flip-flop”. P4-ATPases act as flippases, which translocate phospholipids from the exoplasmic to the cytoplasmic leaflet.

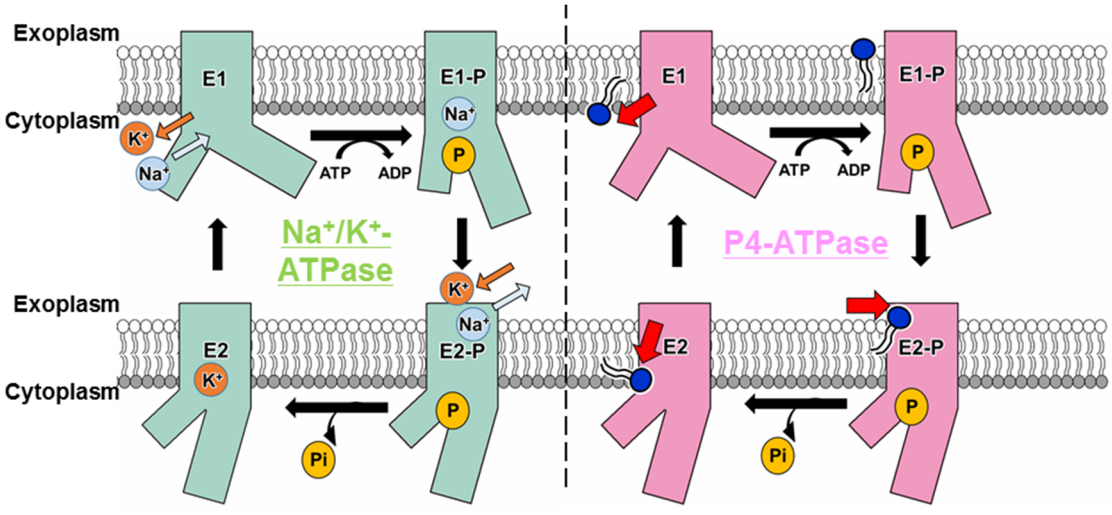

Fig. 0-2. A schematic representation of P4-ATPase reaction cycle.

The reaction cycle of P4-ATPases (*right*) is based on the Post–Albers scheme for other P-type ATPases, such as Na^+/K^+-ATPase (*left*) and Ca^{2+}-ATPase. The phosphoryl group transfer from ATP to an Asp residue converts E1 state to the phosphorylated E1–P state. The phosphorylated E2–P state then forms, and phospholipids bind from the exoplasmic leaflet. The hydrolysis of the phosphorylated Asp leads to E2 state and then to E1 state, translocating phospholipids to the cytoplasmic leaflet.

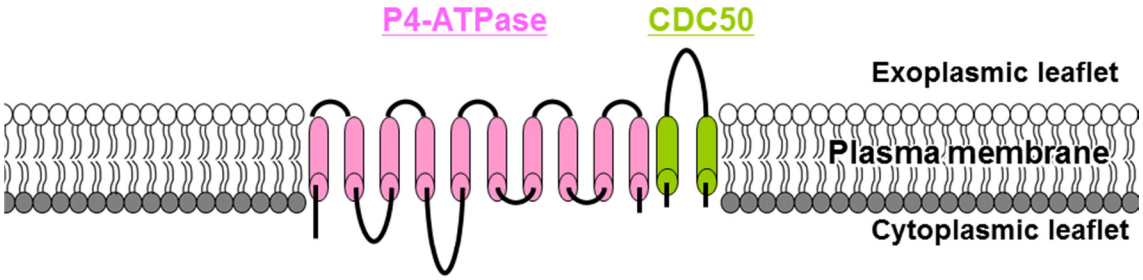

	Human		Yeast	
class	P4-ATPase	CDC50 subunit	P4-ATPase	CDC50 subunit
1a	ATP8A1, ATP8A2	CDC50A	Drs2p	Cdc50p
1b	ATP8B1 ATP8B2, ATP8B4 ATP8B3 (testis)	CDC50A/B CDC50A ?(CDC50C(testis))		
2	ATP9A, ATP9B	-	Neo1p	-
3	-		Dnf1p, Dnf2p	Lem3p
4	-		Dnf3p	Crf1p
5	ATP10A, ATP10B, ATP10D	?		
6	ATP11A, ATP11B, ATP11C	CDC50A		

Fig.0-3. Mammalian and yeast P4-ATPases and CDC50 proteins.

P4-ATPases, except for ATP9A and ATP9B, form heteromeric complexes with CDC50 proteins. The interaction of P4-ATPases with proper CDC50 proteins is necessary for their exit from the ER.

ABBREVIATIONS

ATP	adenosine triphosphate
BSA	bovine serum albumin
CD147	cluster of differentiation 147
CDC50	cell division control protein 50
cDNA	complementary deoxyribonucleic acid
DSP	dithiobis[succinimidylpropionate]
ECM	extracellular matrix
EDTA	ethylenediaminetetraactic acid
EEA1	early endosomal antigen 1
ER	endoplasmic reticulum
FBS	fetal bovine serum
HA	hemagglutinin
HBSS	Hank's balanced salt solution
Lamp-1	lysosome-associated membrane protein 1
MHC-I	major histocompatibility complex 1
mRNA	messenger RNA
NBD	nitrobenzoxadiazole
P4-ATPase	type IV P-type ATPase
PBS	phosphate buffered saline
PC	phosphatidylcholine
PCR	polymerase chain reaction
PE	phosphatidylethanolamine
PFIC	progressive familial intrahepatic cholestasis
PIP_2	phosphatidylinositol 4,5-bisphsphate
PS	phosphatidylserine
RNA	ribonucleic acid
RNAi	RNA interference

RPE	retinal pigment epithelial
RT-PCR	reverse transcription PCR
SDS-PAGE	sodium dodecyl sulfate-polyacrylamide gel electrophoresis
siRNA	small interfering RNA
SM	sphingomyelin
TfnR	transferrin receptor
TM	transmembrane
WT	wild-type

Chapter 1: Subcellular localization of class 5 P4-ATPases and requirement of CDC50 proteins for their localization

ABSTRACT

Type IV P-type ATPases (P4-ATPases) are phospholipid flippases that translocate phospholipids from the outer leaflet to the inner leaflet of lipid bilayers, and most of them form heteromeric complexes with CDC50 proteins (16-20). The human genome encodes 14 P4-ATPases and three CDC50 proteins. In the previous study, our laboratory showed that class 1 and 6 P4-ATPases require CDC50 proteins for their exit from the endoplasmic reticulum (ER) and localize to the plasma membrane or to cellular organelles. In contrast, class 2 P4-ATPases are able to exit the ER without the need of their interaction with CDC50 proteins (20). However, the interaction with CDC50 proteins and the subcellular localization of class 5 P4-ATPases (ATP10A, ATP10B, and ATP10D) are poorly understood. In this study, I revealed that the localization of class 5 P4-ATPases to the plasma membrane (ATP10A and ATP10D) and late endosomes (ATP10B) requires an interaction with CDC50A. Depletion of endogenous CDC50A caused ATP10A and ATP10D to be retained at the ER, instead of being delivered to the plasma membrane. Moreover, I found that a chimeric ATP10 protein, in which the N-terminal cytoplasmic region of ATP10A was replaced with the corresponding region of ATP10B, was localized exclusively to late endosomes. On the other hand, a chimeric ATP10B construct with the N-terminal cytoplasmic region of ATP10D was localized to the plasma membrane. These results demonstrate that class 5 P4-ATPases can exit the ER via their interaction with CDC50A and they contain a signal for subcellular localization in their N-terminal cytoplasmic region.

INTRODUCTION

Lipid bilayers of cellular membranes exhibit asymmetric lipid distributions (1-3). For example, in the plasma membrane of mammalian cells, phosphatidylserine (PS) and phosphatidylethanolamine (PE) are concentrated in the cytoplasmic leaflet, while phosphatidylcholine (PC) and sphingomyelin (SM) are enriched in the extracellular/exoplasmic leaflet. P4-ATPases are phospholipid flippases that translocate phospholipids from the exoplasmic to the cytoplasmic leaflet of the lipid bilayer and play essential roles in generation, maintenance, and spatiotemporal regulation of the membrane asymmetry (4, 5).

Most P4-ATPases require an association with CDC50 proteins for their exit from the endoplasmic reticulum (ER) and subsequent subcellular localization (16-20). The yeast *Saccharomyces cerevisiae* expresses five P4-ATPases (Drs2p, Dnf1p, Dnf2p, Dnf3p, and Neo1) and three CDC50 proteins (Cdc50p, Lem3p, and Crf1p). Cdc50p, Lem3p, and Crf1p associate with Drs2p, Dnf1p/Dnf2p, and Dnf3p, respectively (Fig. 0-3) (12, 15). By contrast, Neo1p does not require the association with either Cdc50p or Lem3p (12). The human genome encodes 14 P4-ATPases, which are grouped into some classes on the basis of sequence similarity: class 1a (ATP8A1 and ATP8A2), class 1b (ATP8B1, ATP8B2, ATP8B3, and ATP8B4), class 2 (ATP9A and ATP9B), class 5 (ATP10A, ATP10B, and ATP10D), and class 6 (ATP11A, ATP11B, and ATP11C) (Fig. 0-3). Although mammals have three CDC50 proteins (CDC50A, CDC50B, and CDC50C), CDC50C expression is restricted to spermatocytes and spermatids (Fig. 0-3) (17, 19). Previous studies showed that most class 1 and class 6 P4-ATPases are associated with CDC50A, but not with CDC50B, whereas ATP8B1 interacted with both CDC50A and CDC50B (16-20). Class 2 P4-ATPases does not associate with either CDC50A or CDC50B as Neo1p in yeast (Fig. 0-3) (20). However, the interaction with CDC50 proteins of class 5 P4-ATPases (ATP10A, ATP10B, and ATP10D) remains unknown. It has been suggested that defects in ATP10A or ATP10D are associated with the abnormality of lipid metabolism, such as obesity and diabetes in mice (28, 30, 33), although cellular functions of class 5 P4-ATPases are unknown.

In this chapter, I characterized the subcellular localization of class 5 P4-ATPases and their interaction with CDC50 proteins. I demonstrated that ATP10A

and ATP10D are localized to the plasma membrane, and ATP10B to late endosomes/lysosomes in a CDC50A-depndent manner, and found that their N-terminal cytoplasmic regions harbor a signal for subcellular localization.

RESULTS

CDC50-dependent Subcellular Localization of ATP10A, ATP10B, and ATP10D

I transiently expressed C-terminally HA-tagged class 5 P4-ATPases in HeLa cells, either alone or in combination with N-terminally FLAG-tagged CDC50A or CDC50B (Fig 1-1), and observed their localization. In the absence of exogenous CDC50 expression or in the presence of exogenous CDC50B, all three class 5 P4-ATPases were predominantly localized to the ER, as demonstrated by their almost complete overlap with an ER marker protein, calnexin (Fig.1-1A and B, *a-a"* and *c-c"*). By contrast, in the presence of exogenous CDC50A, ATP10A and ATP10D were localized predominantly on the plasma membrane (Fig. 1-1A and C, *b-b"*), and ATP10B was localized on punctate structures in the cytoplasm (Fig.1-1B, *b-b"*). The perinuclear staining of ATP10A, ATP10B, and ATP10D might reflect proteins *en route* to the plasma membrane in the biosynthetic pathway.

Next, I compared the subcellular localization of these ATPases with organelle marker proteins (Fig. 1-2). ATP10A and ATP10D were colocalized extensively with a plasma membrane marker, CD147 (Fig. 1-2A). On the other hand, the punctate ATP10B staining overlapped with that of a late endosomal/lysosomal marker, Lamp-1 (Fig. 1-2B), but rarely with an early endosomal marker, EEA1, or an early/recycling endosomal marker, TfnR, indicating that ATP10B is localized mainly to late endosomes and lysosomes. ATPase-deficient glutamate-to-glutamine mutants (21, 34) of ATP10A and ATP10D were colocalized with markers for the plasma membrane, whereas an analogous mutant of ATP10B was localized to endosomes/lysosomes (Fig. 1-3) in the presence of exogenous CDC50A, indicating that ATPase activity may not be a prerequisite for their exit from the ER or delivery to their final destinations. Notably, expression of ATP10A, but not ATP10A(E203Q), caused significant changes in cell shape (Fig. 1-2A and Fig. 1-3); I discuss the physiological relevance of this observation in Chapter 2.

Association of ATP10A, ATP10B, and ATP10D with CDC50A

I next investigated whether class 5 P4-ATPases interact physically with CDC50A. To this end, I transiently transfected HeLa cells with expression vectors for

C-terminally HA-tagged P4-ATPase and N-terminally FLAG-tagged CDC50A, prepared total lysate from the transfected cells, immunoprecipitated the lysates with anti-HA antibody, and subjected the immunoprecipitates to immunoblotting with anti-HA or anti-FLAG antibody (Fig. 1-4). Expression of the tagged proteins was confirmed by immunoblotting of total cell lysates (Fig. 1-4, *input*). As shown in the *bottom two panels* in Fig. 1-4A, ATP10A-HA co-immunoprecipitated FLAG-CDC50A but much less efficiently than ATP8B1 and ATP11A; FLAG-CDC50A migrated as a smear in the SDS-polyacrylamide gel, probably due to heterogeneous glycosylation (20). To my surprise, however, FLAG-CDC50A was not co-immunoprecipitated when co-expressed with ATP10B-HA or ATP10D-HA (Fig. 1-4A, *lanes 4* and *5*). These results suggest that the interaction of the ATP10 proteins with CDC50A might be transient or much weaker than that of other P4-ATPases. To overcome this problem, I performed co-immunoprecipitation analysis after treating the cells with a thiol-cleavable cross linker, DSP (Fig. 1-4B). Lysates prepared from the transfected cells were then immunoprecipitated with anti-HA antibody, and subjected to SDS-PAGE under reducing conditions followed by immunoblotting with anti-HA or anti-FLAG antibody (Fig. 1-4B). After the DSP treatment, CDC50A was co-immunoprecipitated with ATP10B and ATP10D (Fig. 1-4B, *lanes 12* and *13*) as well as with ATP10A (*lane 11*). The amount of CDC50A that was co-immunoprecipitated with ATP10D increased dramatically in the presence of DSP (Fig. 1-4, compare *lane 5* with *lane 13*), whereas that co-immunoprecipitated with ATP10A or ATP10B increased slightly. Thus, the interaction between CDC50A and ATP10 proteins, especially ATP10B and ATP10D, may not be as stable as the interaction between CDC50A and other P4-ATPases, such as ATP8B1 and ATP11A. Because nonspecific bands can be detected in the presence of DSP, I made use of a transmembrane protein, ABCB4, an ABC transporter that localizes to the plasma membrane (35), as a negative control and quantified the band intensities. Taken together, these data indicate that CDC50A interacts physically with ATP10 proteins, but with lower affinity than with other P4-ATPases, and is required for their exit from the ER followed by localization to their destinations.

CDC50A Knockdown Induces Mislocalization of ATP10A and ATP10D

I next examined whether endogenous CDC50A is critical for plasma

membrane localization of ATP10A and ATP10D. To this end, I first established cells stably expressing C-terminally HA-tagged ATP10A, ATP10D, ATP8B1 or ATP11A by infection of recombinant retrovirus (immunoblotting data are shown in Chapter 2, Fig. 2-1). Although exogenous expression of CDC50A is required for the proper localization of transiently expressed P4-ATPases, stably expressed P4-ATPases were detected at the plasma membrane in the absence of exogenous CDC50A expression, indicating that the endogenous CDC50A level was sufficient for the localization of the P4-ATPases due to their moderate expression levels (Fig. 1-5A, siLacZ). I knocked down endogenous CDC50A by RNAi in these cells and confirmed specific and efficient knockdown of CDC50A by RT-PCR (Fig. 1-5B). CDC50A depletion caused mislocalization of ATP10A, ATP10D, ATP8B1 and ATP11A to the ER, overlapping with calnexin (Fig. 1-5A, siCDC50A). These observations strongly support the idea that endogenous CDC50A is required primarily for the ER exit and plasma membrane localization of ATP10A, ATP10D, ATP8B1, and ATP11A.

N-terminal Region of ATP10 Harbors Subcellular Localization Signal

Our laboratory previously showed that the N-terminal cytoplasmic region of ATP9B is required for its Golgi localization (20). I hypothesized that the N-terminal cytoplasmic regions of the ATP10 family proteins might be also responsible for their distinct localization; ATP10A and ATP10D to the plasma membrane, and ATP10B to late endosomes/lysosomes (Fig. 1-2). To address this hypothesis, I constructed chimeric proteins of ATP10A and ATP10B, or ATP10D and ATP10B, and transiently expressed them with CDC50A in HeLa cells (Figs. 1-6 and 1-7). The ATP10BA construct, in which the N-terminal cytoplasmic region of ATP10A was replaced with that of ATP10B, no longer localized to the plasma membrane (Fig. 1-6A), but exclusively localized to late endosomes/lysosomes, overlapping with Lamp-1, but not with EEA1 or TfnR (Fig.1-6B). On the other hand, the ATP10DB chimera, in which the N-terminal region of ATP10B was replaced with that of ATP10D, did not localize to endosomes, but was partly delivered to the plasma membrane and some remained in the ER (Fib. 1-7, *bottom panels*). The ATP10AB chimera, in which the N-terminal region of ATP10B was replaced with that of ATP10A, mislocalized to the ER (Fig. 1-7, *middle panels*), suggesting that ATP10AB may fail to fold properly at some point along its biosynthetic

pathway. Taken together, these results suggest that the N-terminal cytoplasmic region of ATP10B contains a signal for late endosomes/lysosomes localization and that of ATP10D contains a signal for the plasma membrane localization.

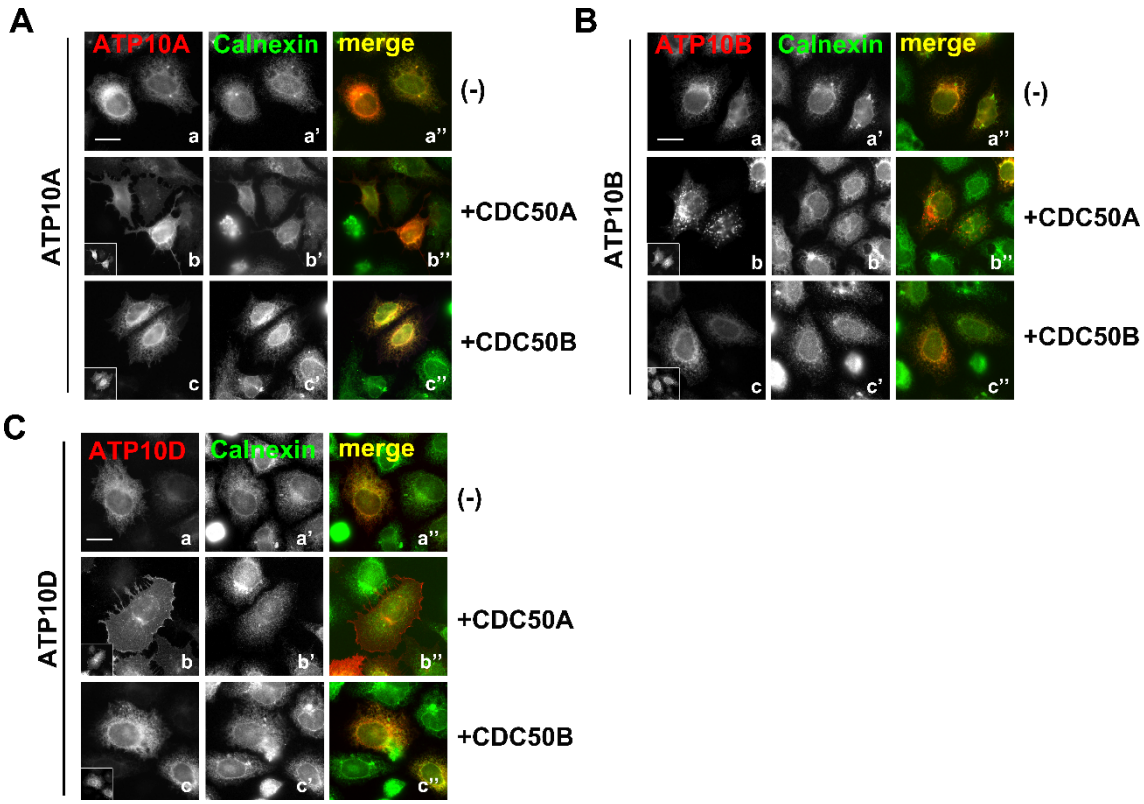

Fig. 1-1. Changes in localization of transiently expressed class 5 P4-ATPases upon co-expression of CDC50.

HeLa cells were transiently co-transfected with an expression vector for C-terminally HA-tagged P4-ATPase and a control vector (*a, a'*, and *a"*) or expression vector for N-terminally FLAG-tagged CDC50A (*b, b'*, and *b"*) or CDC50B *(c, c'*, and *c"*). After 48 h of transfection, the cells were fixed and processed for immunofluorescence microscopy. Cells were stained with anti-HA, anti-FLAG, and anti-calnexin antibodies followed Cy3-conjugated anti-rat, Alexa Fluor 647-conjugated anti-rabbit, and Alexa Fluor 488-conjugated anti-mouse antibodies. *Left insets* show cells expressing FLAG-tagged CDC50A or CDC50B. *Bars*, 20 μm.

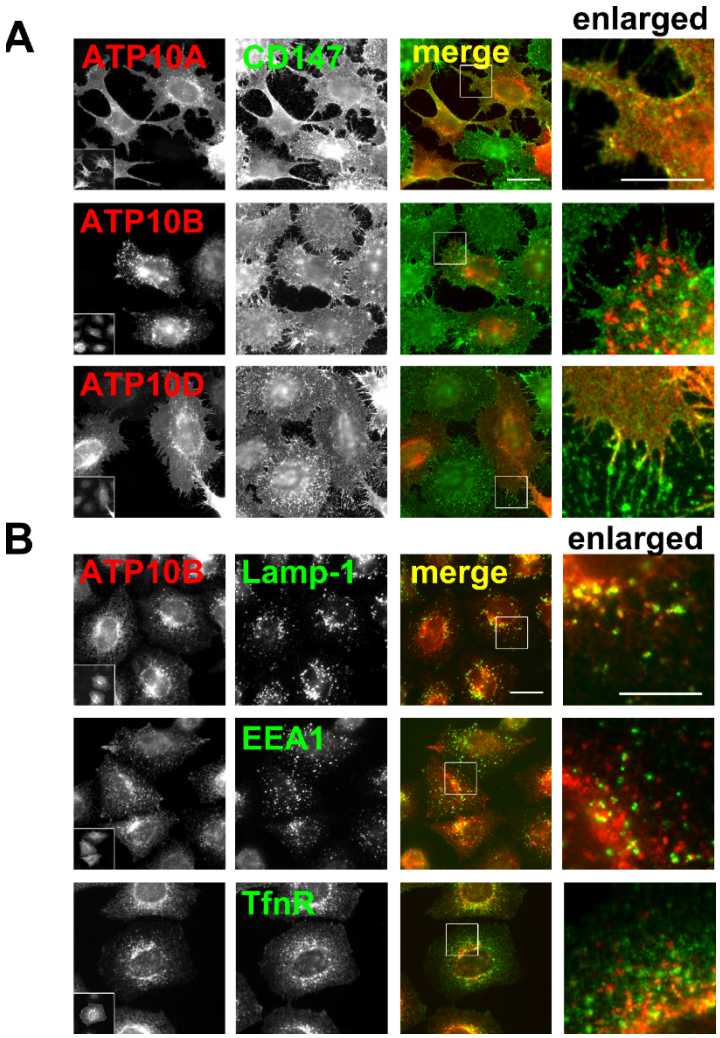

Fig, 1-2. Subcellular localization of class 5 P4-ATPases.

HeLa cells were transiently co-transfected with expression vectors for C-terminally HA-tagged P4-ATPase and N-terminally FLAG-tagged CDC50A. After 48 h of transfection, the cells were fixed and processed for immunofluorescence analysis. *A*, For plasma membrane staining, the cells were incubated with Alexa Fluor 488-conugated anti-CD147 antibody to label the cell surface prior to fixation. The fixed cells were permeabilized and incubated with anti-HA and anti-FLAG antibodies followed by Cy3-conjugated anti-rat and Alexa Fluor 647-conjugated anti-rabbit antibodies. *B*, The fixed cells were stained with antibodies against HA or FLAG and Lamp-1, EEA1, or TfnR, as indicated, followed by Cy3-conjugated anti-rat, Alexa Fluor 647-conjugated anti-rabbit, and Alexa Fluor 488-conjugated anti-mouse antibodies. Right panels represent enlarged images of the boxed regions. *Left insets* show cells expressing FLAG-tagged CDC50A. *Bars*, 20 μm. *Bars* in enlarged images, 10 μm.

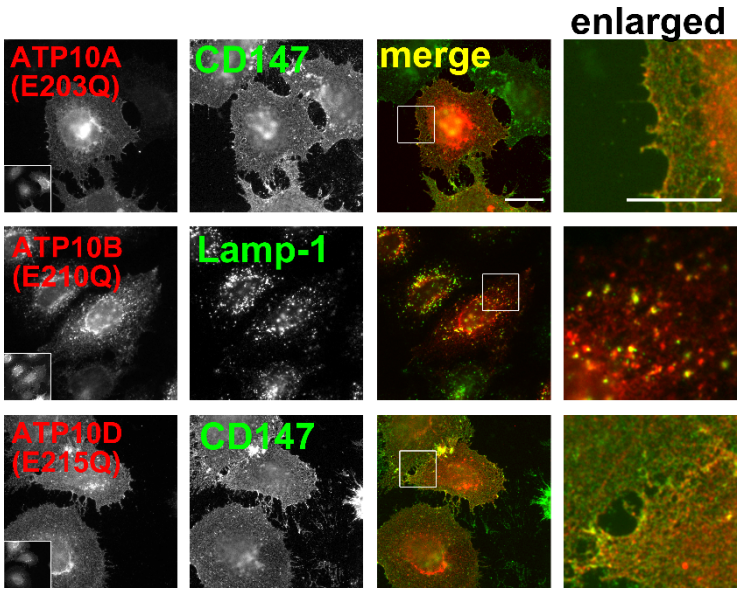

Fig. 1-3. Localization of the ATPase-deficient mutants of class 5 P4-ATPases.

HeLa cells were transiently co-transfected with an expression vector for a glutamate mutant of P4-ATPase with a C-terminal HA tag and for N-terminally FLAG-tagged CDC50A. After 48 h of transfection, the cells were fixed and processed for immunofluorescence microscopy. For plasma membrane staining, cells were incubated with Alexa Fluor 488-conugated anti-CD147 antibody to label the surface prior to fixation. The fixed cells were permeabilized and incubated with anti-HA and anti-FLAG antibodies followed by Cy3-conjugated anti-rat and Alexa Fluor 647-conjugated anti-rabbit antibodies. Alternatively, fixed cells were stained with antibodies against HA or FLAG and Lamp-1 followed by Cy3-conjugated anti-rat, Alexa Fluor 647-conjugated anti-rabbit, and Alexa Fluor 488-conjugated anti-mouse antibodies. Right panels represent enlarged images of the boxed regions. *Left insets* show cells expressing FLAG-tagged CDC50A. *Bar*, 20 μm. *Bar* in enlarged image, 10 μm.

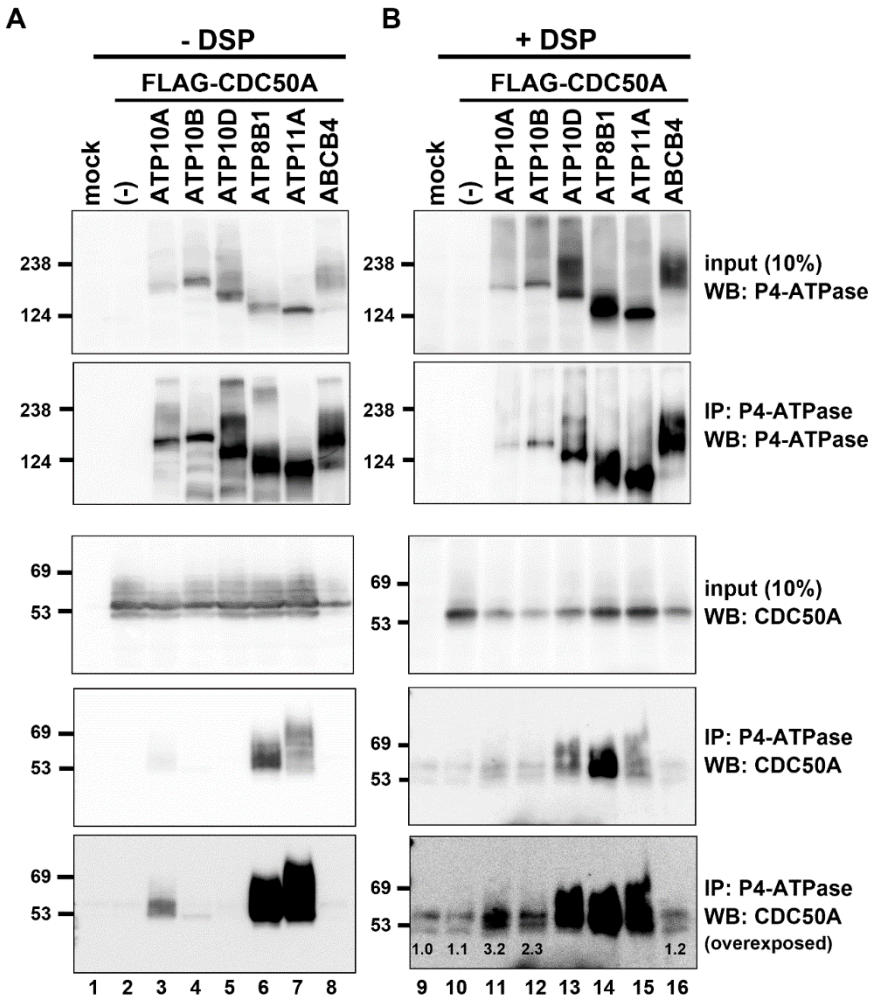

Fig. 1-4. Co-immunoprecipitation analysis to detect interactions between P4-ATPases and CDC50 proteins.

HeLa cells were transfected with an expression vector for FLAG-CDC50A, either alone (*lanes* 2 and 10) or in combination with an expression vector for HA-tagged P4-ATPases or HA-tagged ABCB4 (*lanes* 8 and 16). In mock lanes (*lanes* 1 and 9), HeLa cells were transfected with an empty vector in the absence (A) or presence (B) of cross-linker DSP as indicated. After 48 h of transfection, the cells were mock-treated with dimethyl sulfoxide (A) or treated with DSP (B), lysed, and immunoprecipitated with anti-HA antibody. Bound material and 10% of input were subjected to SDS-PAGE and immunoblotting using anti-HA or anti-FLAG antibody. The numerical values shown in the bottom panel of B are the relative band intensities of co-immunoprecipitated CDC50A when the band intensity in the mock lane is expressed as 1.0.

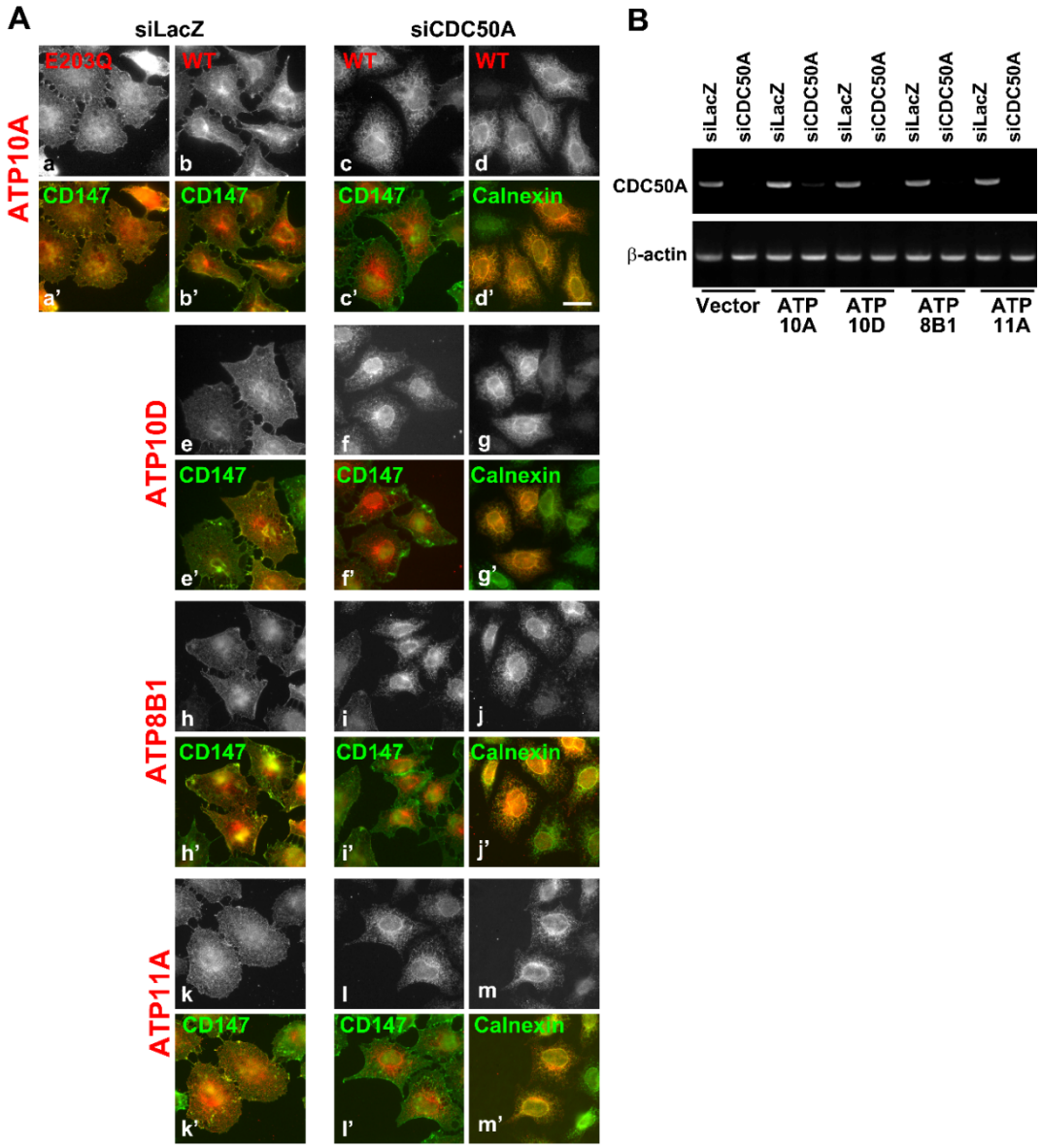

Fig.1-5. Depletion of CDC50A abolishes the plasma membrane localization of P4-ATPases.

A, HeLa cells stably expressing HA-tagged ATP10A, ATP10D, ATP8B1, and ATP11A were treated with a pool of siRNAs targeting LacZ or CDC50A. After 72 h, cells were fixed and processed for immunofluorescence analysis. For ER staining, the fixed and permeabilized cells were incubated with anti-HA and anti-calnexin antibodies followed by Cy3-cojugated anti-rat and Alexa Fluor 488-conjugated anti-mouse antibodies. For plasma membrane staining, cells were treated as described in the legend for Fig. 1-2. *Bar*, 20 μm. *B*, siRNA-treated cells were lysed to isolate total RNAs, which were processed for RT-PCR.

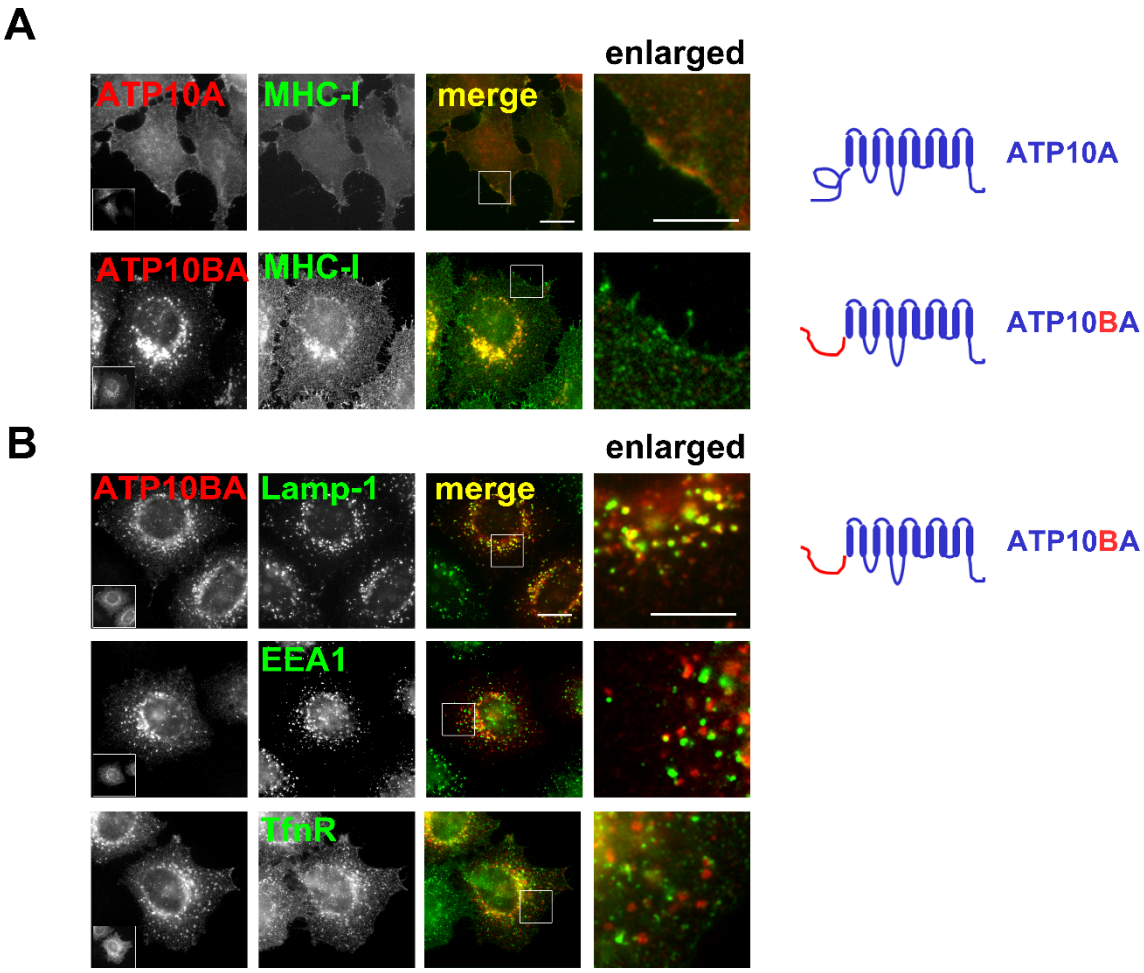

Fig. 1-6. The N-terminal cytoplasmic region of ATP10B harbors a signal for late endosomes/lysosomes localization.

HeLa cells were transiently co-transfected with an expression vector for FLAG-CDC50A and C-terminally HA-tagged ATP10A or a chimeric construct (ATP10BA) schematically shown on the right side. After 48 h of transfection, the cells were fixed and processed for immunofluorescence analysis. *A*, For plasma membrane staining, cells were incubated with anti-MHC-I antibody to label the surface prior to fixation. The fixed cells were permeabilized and incubated with anti-HA and anti-FLAG antibodies followed by Cy3-conjugated anti-rat, Alexa Fluor 647-conjugated anti-rabbit, and Alexa Fluor 488-conjugated anti-mouse antibodies. *B*, The fixed cells were stained with antibodies as described in the legend for Fig. 1-2. Right panels represent enlarged images of the boxed regions. *Left insets* show cells expressing FLAG-tagged CDC50A. *Bars*, 20 μm. *Bars* in enlarged images, 10 μm.

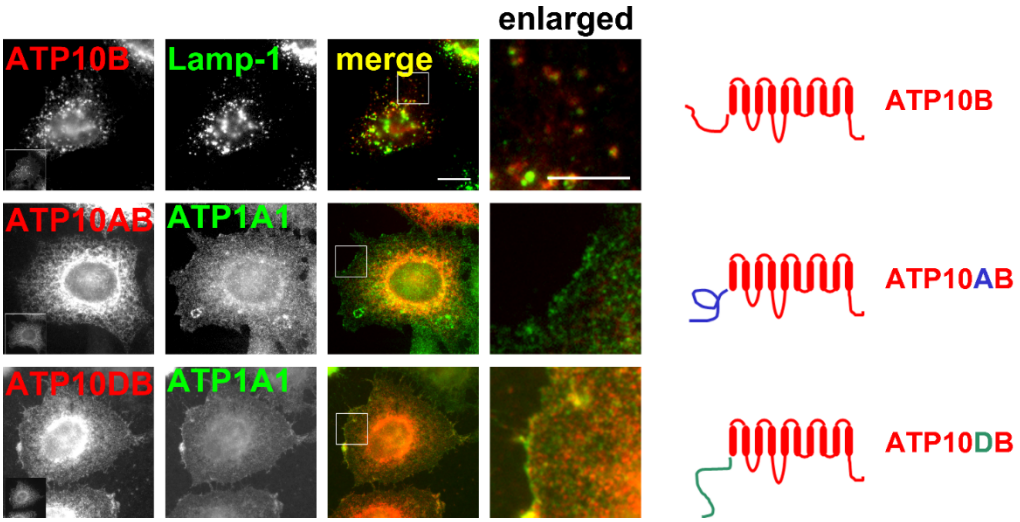

Fig. 1-7. Localization of chimeric constructs of ATP10AB and ATP10DB.

HeLa cells were transiently co-transfected with an expression vector for FLAG-CDC50A and C-terminally HA-tagged ATP10B or a chimeric construct (ATP10AB or ATP10DB) schematically shown on the right side. Cells were fixed and stained with antibodies against HA or FLAG and ATP1A1 (marker for the plasma membrane) followed by Cy3-conjugated anti-rat, Alexa Fluor 488-conjugated anti-rabbit, and Dylight 649-conjugated anti-mouse antibodies. Right panels represent enlarged images of the boxed regions. *Left insets* show cells expressing FLAG-tagged CDC50A. *Bar*, 20 μm. *Bar* in enlarged image, 10 μm.

DISCUSSION

CDC50 proteins are indispensable for the localization of class 1 (ATP8A1, ATP8A2, ATP8B1, ATP8B2, and ATP8B4) and class 6 (ATP11A, ATP11B, and ATP11C) P4-ATPases to cellular compartments (17-20). In this chapter, I demonstrated that class 5 P4-ATPases (ATP10A, ATP10B, and ATP10D) require an interaction with CDC50A, but not CDC50B, for their exit from the ER and localization to specific cellular compartments where they may exert their functions (Fig. 1-1 and Fig. 1-2).

Class 5 P4-ATPases (especially ATP10B and ATP10D) may interact with CDC50A with lower affinity than that of ATP8B1 or ATP11A (Fig. 1-4). Even if the interaction of ATP10 proteins with CDC50A is not as strong as that of ATP8B1 or ATP11A, the interaction is critical for the localization of class 5 P4-ATPases to their final destinations: the plasma membrane for ATP10A and ATP10D and late endosomes/lysosomes for ATP10B (Fig. 1-1 and 1-2). When P4-ATPases were stably expressed in HeLa cells by infection of recombinant retroviral vectors, ATP10A, ATP10D, ATP8B1, and ATP11A were localized to their final destinations in the absence of exogenous CDC50A expression (Fig. 1-1 and Fig. 1-5). This result suggests that endogenous CDC50A might be sufficient for the localization of the P4-ATPases due to their moderate expression levels. In support of this, ATP10A, ATP10D, ATP8B1, and ATP11A were retained in the ER by depletion of endogenous CDC50A in cells stably expressing these P4-ATPases (Fig. 1-5); in the case of ATP10B, it was not able to localize to late endosomes/lysosomes, even when stably expressed in cells, unless exogenous CDC50A was co-expressed (data not shown). The mislocalizaiton of ATP10B to the ER even in stably expressing cells might be due to higher protein expression than other P4-ATPases and/or the lower affinity of ATP10B to CDC50A than other P4-ATPases.

I found that the distinct subcellular localization of ATP10A/ATP10D to the plasma membrane and ATP10B to late endosomes/lysosomes could be attributed to their N-terminal cytoplasmic regions. The ATP10BA chimera was localized exclusively to late endosomes/lysosomes, but not to the plasma membrane (Fig. 1-2 and Fig. 1-6), whereas the ATP10DB chimera was delivered to the plasma membrane, but no longer localized to endosomes (Fig. 1-7). These results indicate that the N-terminal

cytoplasmic region of ATP10B contains a signal for the endosomal localization and that of ATP10D harbors a signal for the plasma membrane localization. The fact that ATP9B (class 2 P4-ATPase) possesses a Golgi localization signal in its N-terminal cytoplasmic region (20), it would be a common mechanism by which the N-terminal cytoplasmic region may determine the localization of P4-ATPases. Therefore, it is an important challenge to identify factors that interact with the N-terminal regions of the ATP10 family proteins for understanding their localization mechanisms.

In summary, nine mammalian P4-ATPases (ATP8A1, ATP8A2, ATP8B1, ATP8B2, ATP8B4, ATP10A, ATP10D, ATP11A, and ATP11C) and three of 5 yeast P4-ATPases (Dnf1p, Dnf2p, and Dnf3p) are localized mainly to the plasma membrane (11, 20, 36), suggesting the importance of regulation of the phospholipid distribution at the plasma membrane. However, I cannot exclude the possibility that these P4-ATPases cycle between intracellular compartments and the plasma membrane, and play a role in the intracellular compartments. The change in transbilayer lipid composition at the plasma membrane mediated by P4-ATPases is involved not only in the regulated exposure of PS in apoptotic cells but also in membrane dynamics required for many cellular functions, such as cytokinesis, cell migration, and cell adhesion.

Chapter 2: Flippase activity and substrate specificity of ATP10A and its involvement in the plasma membrane dynamics

ABSTRACT

Our laboratory previously showed that ATP11A and ATP11C have flippase activity toward aminophospholipids (PS and PE), and ATP8B1 and ATP8B2 have flippase activity toward PC in the plasma membrane (21). I found that exogenous expression of ATP10A, but not its ATPase-deficient mutant ATP10A(E203Q), dramatically increased flipping of PC, but not PS or PE. Depletion of CDC50A abrogated the increased PC flipping activity observed by exogenous expression of ATP10A. These results demonstrate that ATP10A specifically flips PC at the plasma membrane. Importantly, expression of ATP10A, but not ATP10A(E203Q), dramatically altered the cell shape, decreased cell size, and delayed cell adhesion and cell spreading onto the extracellular matrix. Moreover, expression of ATP10A increased the rate of β1-integrin endocytosis. These results suggest that enhanced PC flipping activity due to exogenous ATP10A expression alters the transbilayer lipid balance at the plasma membrane, which may cause a change in cell morphology and in dynamic state of integrin, resulting in delayed cell adhesion and cell spreading. In addition, I found that ATP10A is endogenously expressed in limited cell lines, especially in highly invasive cells, suggesting that PC flipping by ATP10A may be involved in the plasma membrane dynamics during cell migration and/or invasion.

INTRODUCTION

The lipid bilayer of cellular membranes exhibit asymmetric lipid distributions. In mammalian cells, the aminophospholipids, PS and PE, are abundant in the cytoplasmic leaflet, whereas PC and SM are enriched in the exoplasmic leaflet. P4-ATPases translocate phospholipids from the exoplasmic to the cytoplasmic leaflet and play a role in spatiotemporal regulation of transbilayer phospholipid distribution.

Yeast cells express five P4-ATPases, Drs2p, Dnf1p, Dnf2p, Dnf3p, and Neo1p. Drs2p and Dnf1p/Dnf2p, flip NBD-labeled PS (NBD-PS) at the Golgi complex and NBD-PC and NBD-PE at the plasma membrane, respectively (11, 36). A recent study implicated Neo1p in concentrating PE in the cytosolic leaflet of the Golgi and endosomes (37). The yeast P4-ATPases are all involved in vesicular transport in the secretory and endocytic pathways, albeit at different stages (38).

Although comprehension of the enzymatic properties of P4-ATPases is essential for understanding their physiological functions, flippase activities and substrate specificities of mammalian P4-ATPases has been poorly characterized. Recently, the flippase activities and cellular functions of some mammalian P4-ATPases were explored. Our laboratory showed that ATP11A and ATP11C can flip NBD-PS and -PE, and ATP8B1 and ATP8B2 preferentially flip NBD-PC at the plasma membrane (21). During apoptosis, ATP11C undergoes caspase-mediated cleavage and is consequently inactivated, resulting in PS exposure on the cell surface (27). Mutations in the ATP8B1 gene cause progressive familial intrahepatic cholestasis1 (PFIC1) (22, 23). The phenotypes of some PFIC1 patients result from impairment of PC-flippase activity of ATP8B1 (21). Lee *et al.* showed that PS flipping by ATP8A1 is required for the recruitment of the membrane fission protein to recycling endosomes and Kato *et al.* showed that PE flipping activity by ATP8A1 at the plasma membrane is required for cell migration (39, 40). Tanaka *et al.* demonstrated that ATP9A localized to early/recycling endosomes plays an important role in protein transport from endosomes to the plasma membrane (41). Heterozygous deletion of ATP10A in mice causes diet-induced obesity, type 2 diabetes, and nonalcoholic fatty liver disease, implicating ATP10A in obesity-related metabolic abnormalities (28). ATP10A is also implicated in regulation of insulin-stimulated glucose uptake (29, 30). *ATP10D* variants are

associated with myocardial infarction in German population and with atherosclerosis in Japanese elderly population (31, 32). However, the flippase activities, substrate specificities and cellular functions of class 5 P4-ATPases (ATP10A, ATP10B, and ATP10D) remain unknown.

In the previous chapter, I revealed that ATP10A and ATP10D are localized to the plasma membrane in a CDC50A-dependent manner. Therefore, I tried to measure their flippase activities since the established method in our laboratory is able to detect the flippase activity at the plasma membrane. In this study, I found ATP10A exhibited flippase activity toward NBD-PC. Moreover, enhanced PC-flipping activity due to exogenous ATP10A expression caused changes in cell shape and cell size, and inhibited cell adhesion and spreading onto the extracellular matrix (ECM). In addition, expression of ATP10A increased the rate of β1-integrin endocytosis.

RESULTS

ATP10A Translocates NBD-PC

In the previous study, our laboratory demonstrated the flippase activities and substrate specificities of plasma membrane-localizing P4-ATPases ATP8B1, ATP8B2, ATP11A, and ATP11C using NBD-labeled phospholipids (21). ATP11A translocates aminophospholipids (PS and PE) (Fig. 2-2B and C), whereas ATP8B1 preferentially flips PC (Fig. 2-2A). Here, I investigated the flippase activities of ATP10A and ATP10D, which are also localized to the plasma membrane (see Chapter 1, Fig. 1-1). To this end, I made use of cells stably expressing ATP10A, ATP10A(E203Q), or ATP10D which were established by infection of recombinant retrovirus (Chapter 1). The expression of P4-ATPases in these cells were confirmed by immunoblotting (Fig. 2-1) and immunofluorescence (see Chapter 1, Fig. 1-5). Stably expressed ATP10A and ATP10D were detected at the plasma membrane in the absence of exogenous CDC50A as described in Chapter 1 (Fig. 1-3).

Intriguingly, cells stably expressing ATP10A exhibited a highly selective flippase activity toward NBD-PC (Fig. 2-2, A and E) but no activities toward any other NBD-phospholipids that I examined (Fig. 2-2, B-D and F-H). Furthermore, the PC flipping activity of ATP10A-expressing cells was much higher than that of cells stably expressing ATP8B1 (Fig. 2-2A). By contrast, cells stably expressing ATP10A(E203Q), an ATPase-deficient mutant, did not exhibit significant flippase activity toward NBD-PC (Fig. 2-2A), although the expression level of ATP10A(E203Q) was comparable with that of ATP10A (Fig. 2-1). The results indicate that the increase in translocation of NBD-PC from the exoplasmic to the cytoplasmic leaflet in ATP10A-expressing cells was dependent on the ATPase cycle of ATP10A. I also examined the time course of flippase activities in ATP10A-expressing cells (Fig. 2-2, E-H). HeLa cells stably expressing ATP10A exhibited a dramatic increase in the amount of BSA-non-extractable NBD-PC as compared with parental HeLa cells (Fig. 2-2E). By contrast, the time-dependent increase in the amount of NBD-PS, NBD-PE, or NBD-SM in ATP10A-expressing cells did not differ significantly from that in parental cells (Fig. 2-2, F-H).

I did not detect flippase activity of ATP10D toward any of the

NBD-phospholipids I examined (Fig. 2-2, A-D). ATP10D might have flippase activity toward other lipids, although I cannot exclude the possibility that the flippase activity of ATP10D was undetectable due to its low specific activity and/or low expression level in the stable cells (Fig. 2-1).

To confirm that the PC flipping activity observed in the ATP10A-expressing cells was indeed due to ATP10A expression, I treated cells stably expressing ATP10A or ATP10A(E203Q) with siRNAs targeting ATP10A and examined their flippase activities. Immunoblot analysis revealed that the expression level of ATP10A or ATP10A(E203Q) was significantly reduced in knockdown cells (Fig. 2-3A). In parallel with the decrease in ATP10A expression levels, the flipping activity toward PC was dramatically decreased by treatment of the cells with ATP10A siRNA but not control siRNAs (siRNAs for LacZ) (Fig. 2-3B), indicating that the observed PC flipping activity could be attributed to ATP10A expression. By contrast, ATP10A depletion did not affect the uptake of other NBD-phospholipids (Fig. 2-3, C-E). Notably, depletion of ATP10A in control HeLa cells did not decrease basal PC flipping activity (Fig. 2-3B), because endogenous ATP10A was not expressed in HeLa cells (Fig. 2-10); I discuss later about the endogenous expression of ATP10A in various cell lines.

Co-expression of CDC50A, but not CDC50B, with ATP10A or ATP11A Increases the Phospholipid Flipping Activities

ATP10A, ATP8B1, and ATP11A are localized to the plasma membrane in a CDC50A-dependent manner (see Chapter 1) (20). Therefore, I asked whether the phospholipid flipping activities of ATP10A, ATP8B1, and ATP11A are dependent on CDC50A as well. To this end, I transiently co-expressed ATP10A, ATP8B1, and ATP11A with either CDC50A or CDC50B in HeLa cells and subjected the cells to the flippase assay. Exogenous expression of ATP10A alone moderately increased flippase activity toward NBD-PC relative to vector-transfected control cells (Fig. 2-4A, *gray bar*), suggesting that some fraction of ATP10A might be transported to the plasma membrane with the aid of endogenous CDC50A. Co-expression of CDC50A with ATP10A further increased the PC flipping activity (Fig. 2-4A, *closed bar*). By contrast, cells co-expressing CDC50B with ATP10A (Fig. 2-4A, *open bar*) exhibited a PC flipping activity comparable to those expressing ATP10A alone (*gray bar*).

Co-expression of ATP11A with CDC50A, but not CDC50B, increased flipping activity toward NBD-PS and NBD-PE (Fig. 2-4B and C). Expression of ATP8B1 tended to increase PC flipping activity, although the effect was not statistically significant (Fig. 2-4A, *gray bar*), and co-expression of ATP8B1 with CDC50A slightly but significantly increased the activity (*closed bar*). The activity of ATP8B1 might be difficult to detect in transiently expressing cells, because the PC flipping activity of ATP8B1 was much lower than that of ATP10A even in stably expressing cells (Fig. 2-2A).

CDC50A Knockdown Abolishes Flippase Activities of ATP10A, ATP8B1, and ATP11A

In the previous chapter, I showed that CDC50A knockdown induced mislocalization of ATP10A, ATP10D, ATP8B1, and ATP11A to the ER (see Chapter 1, Fig. 1-3). I next asked whether the flippase activities of cells stably expressing ATP10A, ATP8B1, or ATP11A were affected by CDC50A depletion. CDC50A depletion reversed the PC flipping activities observed in cells stably expressing ATP10A or ATP8B1 (Fig. 2-5A) and decreased the PS and PE flipping activities observed in ATP11A-expressing cells (Fig. 2-5B and D). These data indicate that these P4-ATPases cannot be transported to the plasma membrane in the absence of CDC50A, resulting in abrogation the phospholipid flipping activities observed in cells stably expressing these P4-ATPases.

Notably, in vector-infected control HeLa cells, depletion of CDC50A markedly decreased PS and PE flipping activities, but barely decreased PC flipping activity (Fig. 2-5A, B, and D, *open bars* in vector). The dramatic decrease in PS flipping activities in cells depleted of CDC50A might be ascribed to failed delivery of endogenous PS-flipping P4-ATPases to the plasma membrane in the absence of CDC50A. These data are compatible with the fact that endogenous PS-flipping activity in HeLa cells is much higher than the activities toward other phospholipids (Fig. 2-2, E-H) (21). Therefore, the high and constitutive PS flipping activities might be required in HeLa cells to prevent the exposure of PS to the outer leaflet and to maintain the asymmetry between the two leaflets of the plasma membrane. On the other hand, the PC flipping event might occur at a very low rate at steady state, or it might be required under specific conditions (such as in response to signals) or in a specific place (such as

the bile canaliculi) (21, 22, 42).

Enhanced PC Flipping Activity Alters Cell Shape and Decreases Cell Size

During the course of my experiments, I noticed that cell shape was significantly altered by overexpression of ATP10A but not that of the ATP10A(E203Q) mutant (Figs.1-1, 1-2, 1-3, and 2-6). As shown in Fig. 2-6A, the shape of cells transiently expressing ATP10A(WT) and CDC50A (Fig. 2-6Ac) was dramatically altered relative to that of control cells (Aa). By contrast, cells transiently expressing ATP10A(E203Q) and CDC50A (Ad) did not exhibit an observable shape change relative to control cells (Aa). To quantitatively show the change in cell shape, I stained the cells with a plasma membrane marker, MHC-I, and quantitated cell areas (Fig. 2-6A and B). The frequency distribution of cell areas revealed that the population of small-sized cells markedly increased upon co-expression of ATP10A and CDC50A (Fig. 2-6Bc). By contrast, the frequency distribution of cell areas in cells co-expressing ATP10A(E203Q) and CDC50A (Fig. 2-6Bd) was not significantly changed relative to control (Ba) or CDC50A-expressing cells (Bd). These results indicate that the change in cell shape and decrease in cell size could be ascribed to enhanced PC flipping activity due to elevated expression of ATP10A at the plasma membrane.

Enhanced PC Flipping Activity Inhibits Cell Adhesion and Spreading

I next asked whether cell adhesion and spreading were altered by ATP10A expression. For this purpose, I examined the efficiency of cell adhesion in cells stably expressing ATP10A and ATP10A(E203Q). Cells detached from the dishes by EDTA treatment were resuspended in medium supplemented with fetal bovine serum (FBS) and seeded onto plastic dishes. After incubation for the indicated times, non-adherent cells were removed by washing with PBS, and adherent cells were stained with crystal violet. The stain was then extracted from cells and quantitated by measuring the absorbance at 570 nm; although the same numbers of cells were seeded, the absorbance was normalized to the DNA content of the seeded cells to achieve a more accurate assessment. As shown in Fig. 2-7, adhesion of ATP10A-expressing cells was delayed relative to the control cells. By contrast, adhesion of ATP10A(E203Q)-expressing cells was not delayed but instead was slightly accelerated. After 60 min of incubation, cell

adhesion was comparable among cells expressing ATP10A or ATP10A(E203Q) and control cells (Fig. 2-7A). Thus, cell adhesion was delayed in cells expressing ATP10A. Notably, the extent of cell spreading at the 60-min time point appeared to be lower in cells expressing ATP10A(WT) (Fig. 2-7B, *middle panel*) relative to control and ATP10A (E203Q)-expressing cells (Fig. 2-7B, *top* and *bottom panels*, respectively). I next asked whether cell spreading was affected by expression of ATP10A. To this end, cells stably expressing ATP10A(WT) or ATP10A(E203Q) were detached from dishes by EDTA treatment, resuspended in serum-free medium, and seeded onto FBS- or fibronectin-coated coverslips. As shown in Fig. 2-8A and C, cells stably expressing ATP10A(WT) spread more slowly onto the FBS- or fibronectin-coated coverslips than control cells and those expressing ATP10A(E203Q) (compare the cells at 60-, 120-, and 180-min time point). I quantitated the areas of the cells at the 180-min time point (Fig. 2-8B and D). The frequency distribution of cell areas revealed that the population of small-sized cells increased significantly upon stable expression of ATP10A(WT) but not ATP10A(E203Q) (Fig. 2-8B and D). Taken together, these observations indicate that the suppression of cell adhesion and spreading observed in cells expressing ATP10A can be ascribed to enhanced PC flippase activity.

Enhanced PC Flipping Activity Increases the Rate of β1-Integrin Endocytosis

I next asked whether ATP10A expression altered the dynamic state of integrins, which are key components for cell adhesion to the ECM via the connection between the cytoskeleton and the ECM, such as fibronectin (43). The function of integrins are regulated by the endocytic trafficking; cycles of endocytosis and recycling control the availability of integrins on the plasma membrane (44). I hypothesized that the inhibition of cell adhesion and spreading by ATP10A expression might be due to the alteration of dynamic state of integrins. To this end, HeLa cells expressing ATP10A were incubated with anti-β1-integrin antibody at 4ºC for 1 h, washed with PBS to remove unbound antibodies, and then incubated at 37ºC for indicated times in the absence of the antibody (Fig. 2-9A). Before fixation, cells were washed with acidic solution to remove residual antibodies on the plasma membrane. I confirmed that the plasma membrane-bound anti-β1-integrin antibody was efficiently removed after washing with acidic solution (Fig. 2-9A, (-) and (+) acid wash at 0-min time point). I

found that the intracellular signals of β1-integrin increased in cells expressing ATP10A(WT) relative to control cells and ATP10A(E203Q) expressing cells at the 15- or 30-min time points (Fig. 2-9A). I quantitated the fluorescence intensity of the intracellular β1-integrin signals at the 15- or 30-min time point (Fig. 2-9B). The amount of internalized β1-integrin were increased in cells expressing ATP10A(WT) but not ATP10A(E203Q) at both time points (Fig. 2-9B), suggesting that enhanced PC flipping activity promotes the endocytosis of β1-integrin. Therefore, the increased PC flipping activity due to exogenous ATP10A expression alters the transbilayer lipid balance at the plasma membrane, which may cause a change in cell morphology and in dynamic state of β1-integrin, resulting in delayed cell spreading and adhesion.

Endogenous ATP10A Is Expressed in Highly Invasive and Motile Cells

To investigate the physiological function of ATP10A, I examined mRNA expression of class 5 P4-ATPases in various cell lines. RT-PCR analysis showed that ATP10D (*third panel*) and CDC50A (*bottom panel*; as positive control) were expressed in all examined cell lines (Fig. 2-10). On the other hand, ATP10A was expressed in limited cell lines, such as MDA-MB-231 and RPE-1 cells (Fig. 2-10A, *top panel*), which are highly motile cells (45, 46). Intriguingly, ATP10A was expressed in a highly invasive breast cancer cell line, MDA-MB-231, but not in a noninvasive breast cancer cell line, MCF-7 (Fig. 2-10) (45). These results suggest a possibility that ATP10A might play a role in cell migration and invasion. ATP10B was expressed in all cell lines but weakly expressed in HeLa and MDA-MB-231 cells (Fig.2-10, *second panel*).

Finally, I asked whether depletion of endogenous ATP10A causes the decrease in basal PC flipping activity in MDA-MB-231 cells. To this end, I knocked down endogenous CDC50A or ATP10A by RNAi in MDA-MB-231 cells, and then examined the flippase activity. I confirmed the specific and efficient knockdown of CDC50A and ATP10A by RT-PCR (Fig. 2-11A). Depletion of CDC50A or ATP10A did not affect basal PC flipping activity (Fig. 2-11B), whereas depletion of CDC50A decreased PS and PE flipping activity in MDA-MB-231 cells (Fig. 2-11C and E) as well as in HeLa cells (Fig. 2-5). These data suggest that ATP10A may remain inactive at steady state in MDA-MB-231 cells. Because PC is abundant in the outer leaflet at steady state, tight regulation of PC-flippase activity might be required for cellular homeostasis.

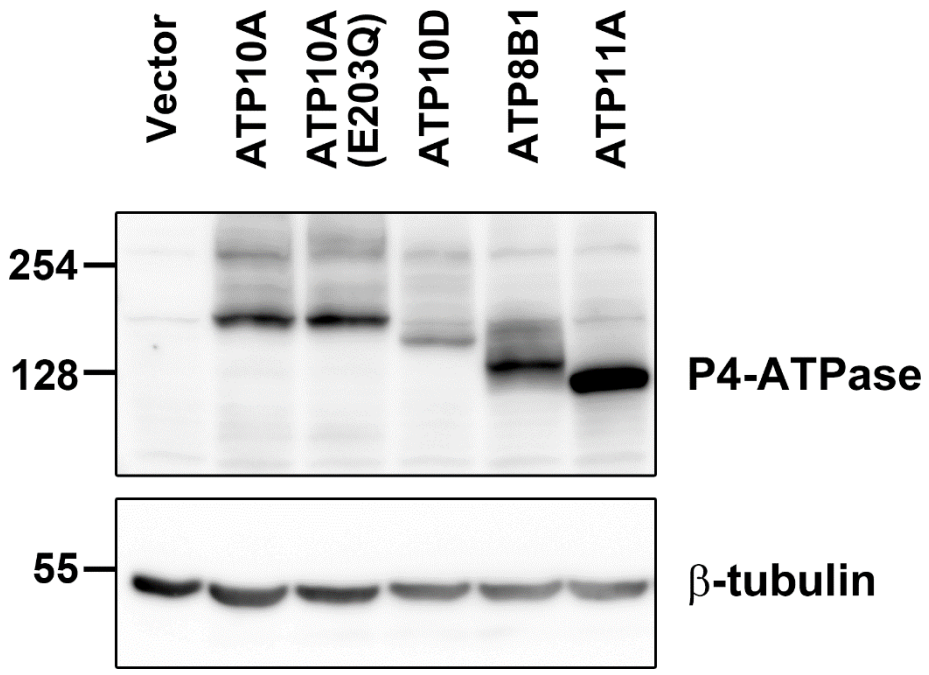

Fig. 2-1. Establishment of HeLa cells stably expressing HA-tagged P4-ATPases

HeLa cells stably expressing HA-tagged P4-ATPases, as indicated, were established by infection of recombinant retrovirus and subsequent selection in the presence of G418. The cells were lysed and subjected to SDS-PAGE and immunoblotting using anti-HA or anti-β-tubulin antibody (as an internal control) to determine the total expression level of the P4-ATPase proteins.

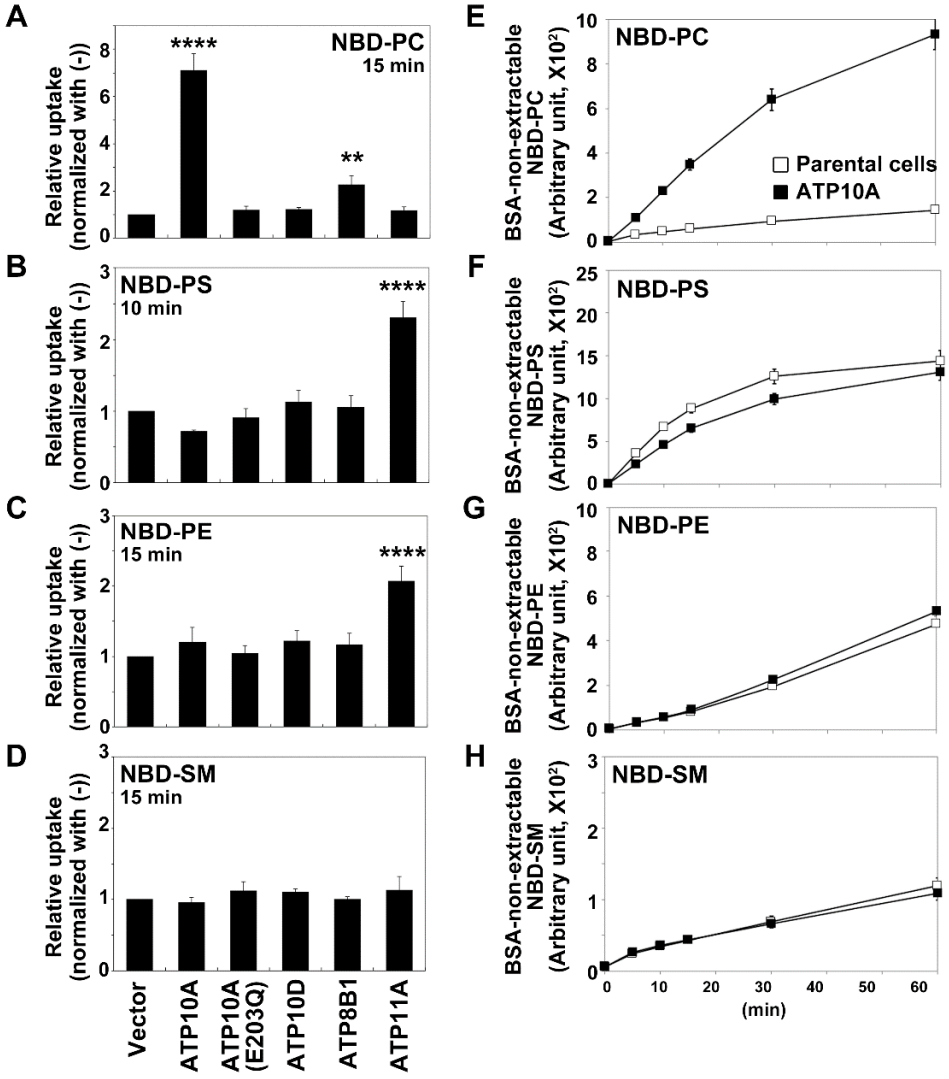

Fig. 2-2. Flippase activities across the lipid bilayer of the plasma membrane in HeLa cells stably expressing ATP10A.

A-D, HeLa cells stably expressing HA-tagged P4-ATPases were incubated with the indicated NBD-lipids at 15°C for the indicated times. After extraction with fatty acid-free BSA, residual fluorescence intensity associated with the cells was determined by flow cytometry. The fold increase in NBD-lipid uptake relative to that in vector-infected control cells is shown. The graphs display averages ± S.D. from three independent experiments (**, $p<0.01$, ****, $p<0.0001$). *E-H*, Parental HeLa cells (open squares) or cells stably expressing ATP10A (closed squares) were incubated with indicated NBD-lipids at 15°C for the indicated times. Graphs display averages ± S.D. from three independent experiments.

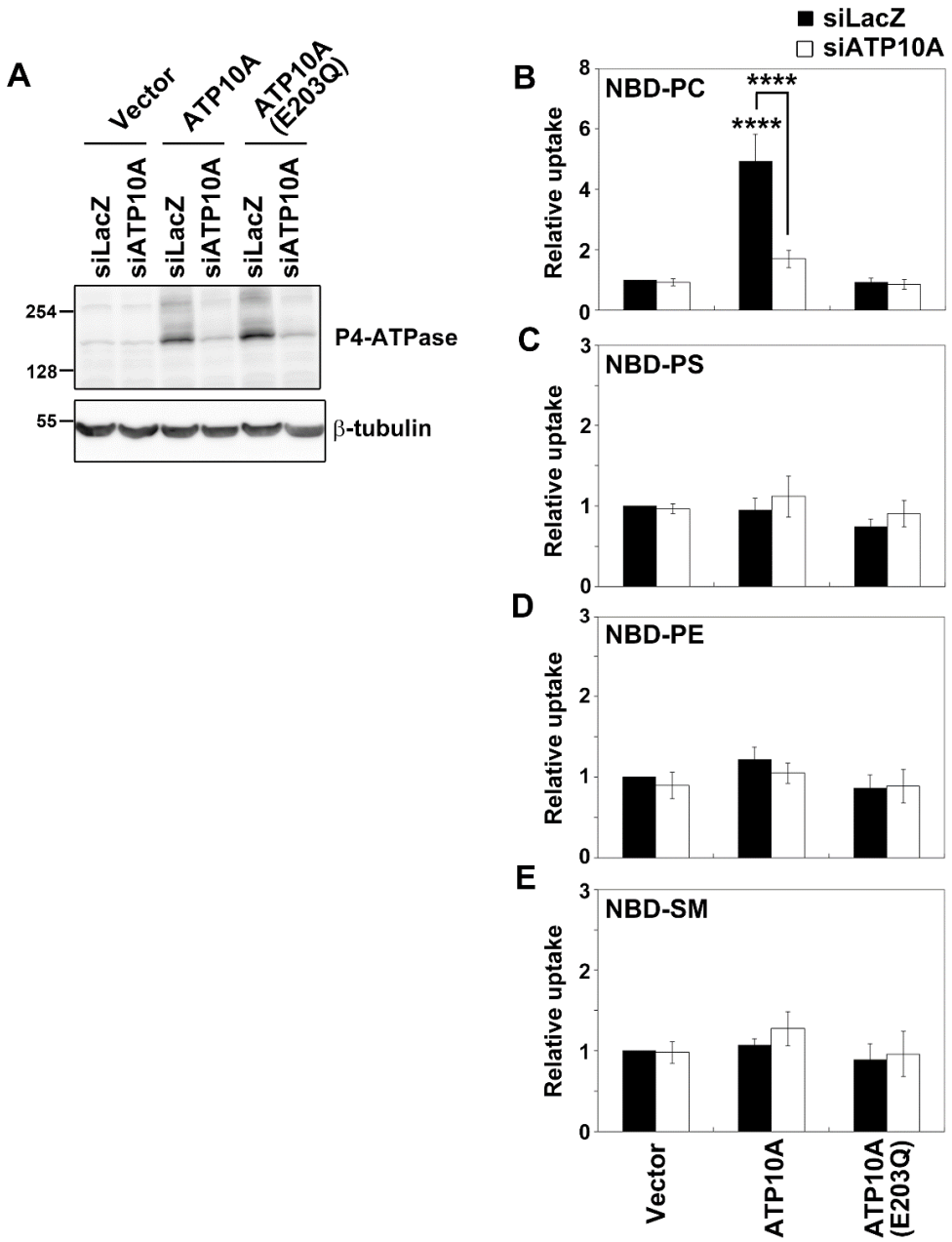

Fig. 2-3. Depletion of ATP10A decreases the PC flipping activity in HeLa cells stably expressing ATP10A.

HeLa cells stably expressing HA-tagged ATP10A or ATP10A(E203Q) were treated with a pool of siRNA for LacZ or ATP10A for 120 h. *A*, Cells were lysed and subjected to SDS-PAGE and immunoblotting using anti-HA or anti-β-tubulin antibody. *B*-*E*, Cells were incubated with indicated NBD-lipids as described in the legend for Fig. 2-2. Graphs display averages ± S.D. from three independent experiments (****, $p<0.0001$).

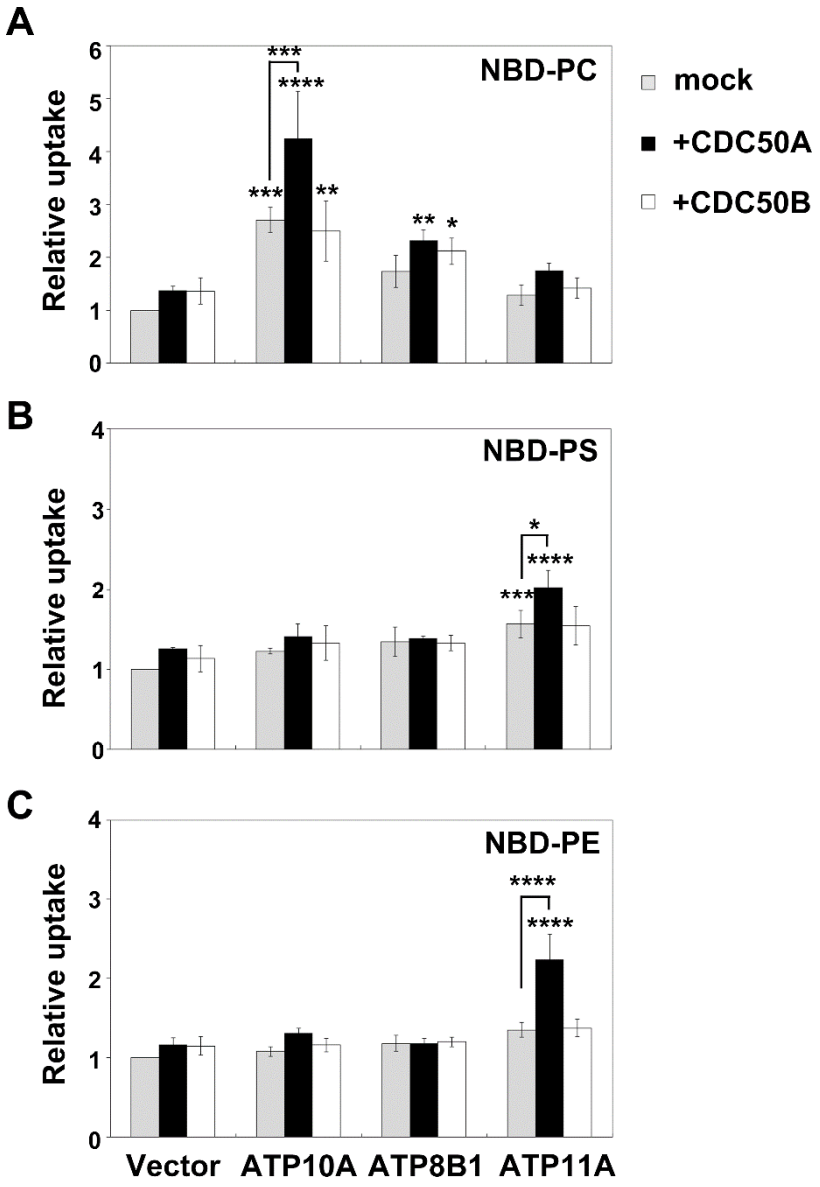

Fig. 2-4. Co-expression of ATP10A with CDC50A, but not CDC50B, increases flippase activities.

HeLa cells were transiently transfected with an expression vector encoding HA-tagged ATP10A, ATP8B1, or ATP11A either alone or together with a vector encoding FLAG-CDC50A or FLAG-CDC50B. After 48 h, the cells were incubated with NBD-lipids as indicated at 15°C, and residual fluorescence intensity associated with cells determined by flow cytometry as described in the legend for Fig. 2-2. The fold increase in NBD-lipid uptake relative to vector-transfected control cells is shown. Graphs display averages ± S.D. from three independent experiments (*, $p<0.05$, **, $p<0.01$, ***, $p<0.001$, ****, $p<0.0001$).

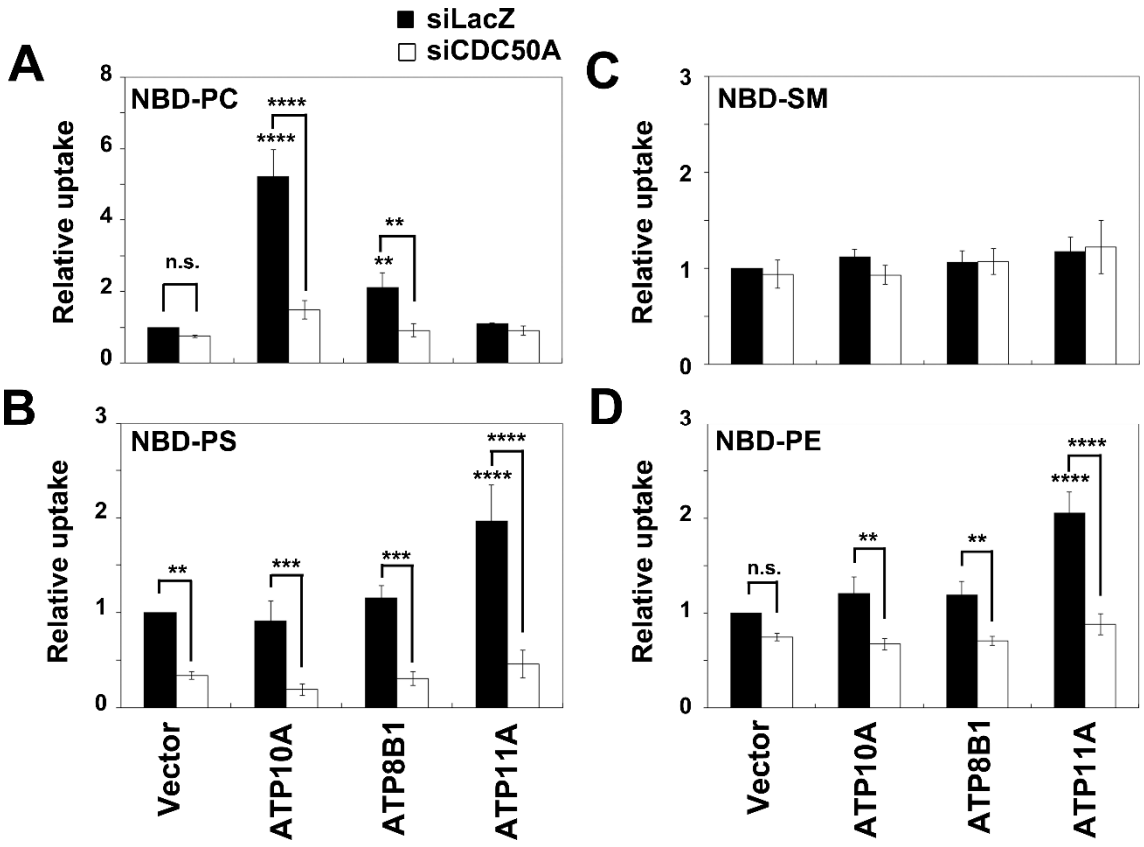

Fig. 2-5. Depletion of CDC50A abolishes the flippase activities of P4-ATPases at the plasma membrane.

Knockdown of CDC50A in HeLa cells stably expressing HA-tagged P4-ATPases are performed as described in the legend for Fig. 1-5. The siRNA-treated cells were incubated with the indicated NBD-lipids at 15°C, and the residual fluorescence intensity associated with the cells was determined by flow cytometry as described in the legend for Fig. 2-2. The fold increase in NBD-lipid uptake compared with vector-infected and siLacZ-treated control cells is shown. Graphs display averages ± S.D. from three independent experiments (**, $p<0.01$, ***, $p<0.001$, ****, $p<0.0001$, n.s., not significant).

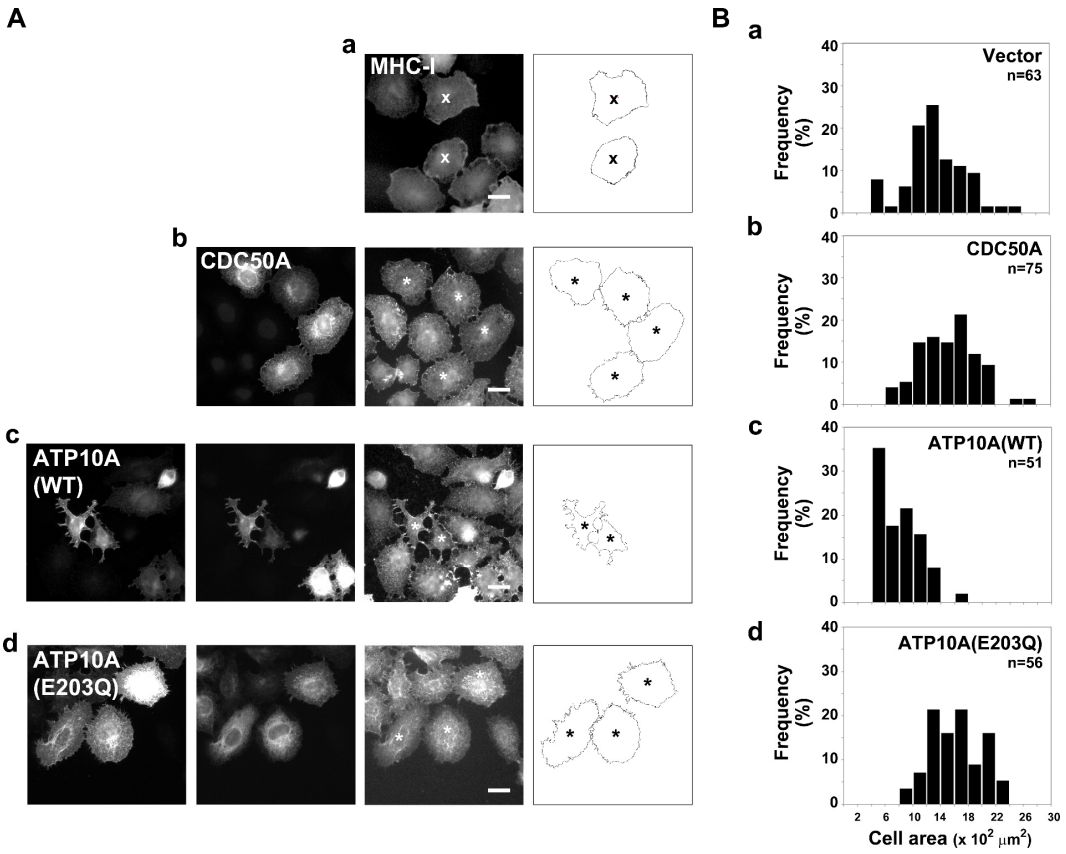

Fig. 2-6. Overexpression of ATP10A causes a change in cell shape and a decrease in cell size.

HeLa cells were transiently transfected with an empty expression vector (*a*) or an expression vector for FLAG-CDC50A (*b*) either alone or in combination with an expression vector for ATP10A-HA (*c*) or ATP10A(E203Q)-HA (*d*). *A*, After 48 h, the cells were stained with anti-MHC-I, anti-HA, and anti-FLAG antibodies as described in the legend for Fig. 1-6. *Bars*, 20 μm. HeLa cells (*a, cross marks*) or cells expressing FALG-CDC50A alone (*b*) or in combination with either ATP10A-HA (*c*) or ATP10A(E203Q)-HA (*d*) (indicated by *asterisks* in right panels) were outlined by setting a threshold for the fluorescence intensities of MHC-I staining. *B*, each cell areas was measured by the ImageJ software, and the frequency distribution of the cell size is shown.

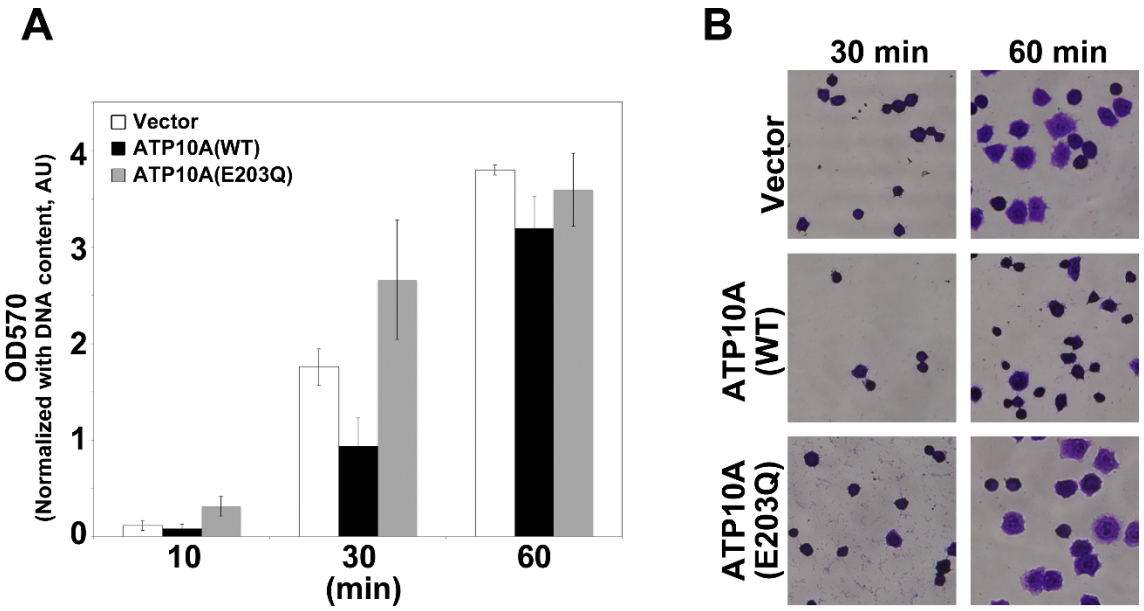

Fig. 2-7. Enhanced PC flipping activity delays cell adhesion.

Adhesion assay was performed using HeLa cells stably expressing ATP10A-HA or ATP10A(E203Q)-HA. Cells were seeded onto a plastic dish and incubated for the indicated times. After washing to remove non-adherent cells, adherent cells were stained with crystal violet. The stain was processed for measurement of absorbance at 570 nm. Graphs display averages ± S.D. from quintuplicates at 570 nm. In *B*, representative images of cells stained with crystal violet are shown.

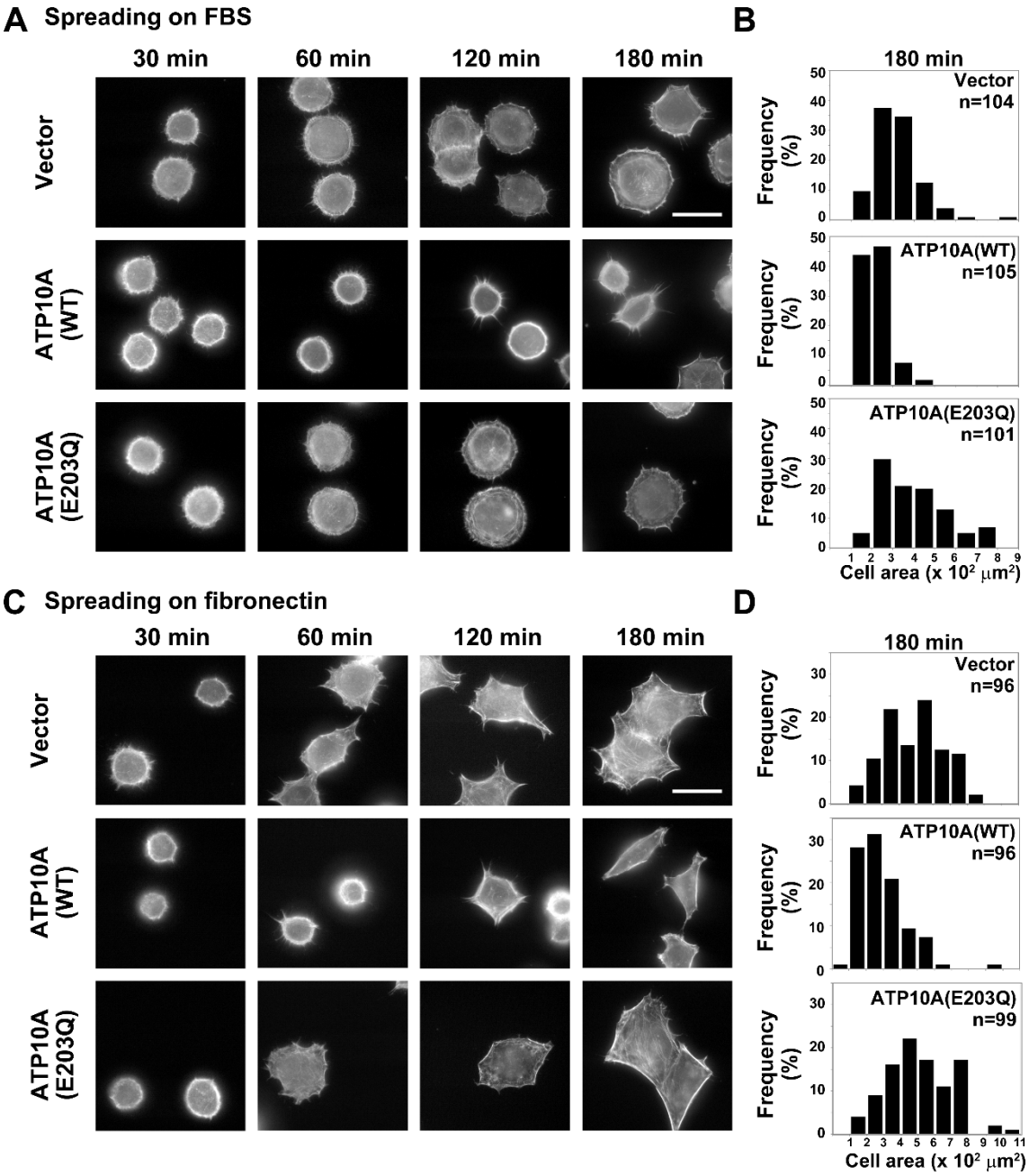

Fig. 2-8. Enhanced PC flipping activity delays cell spreading.

HeLa cells stably expressing ATP10A-HA or ATP10A(E203Q)-HA were processed for the spreading assay. Cells were seeded onto FBS-coated (A and B) or fibronectin-coated (C and D) coverslips and incubated for the indicated times. After fixation and permeabilization, cells were incubated with Alexa Fluor 488-conjugated phalloidin (A and C). *Bars*, 20 μm. B and D, Cell areas were measured by the MetaMorph software, and the frequency of distribution of cell areas at 180 min is shown.

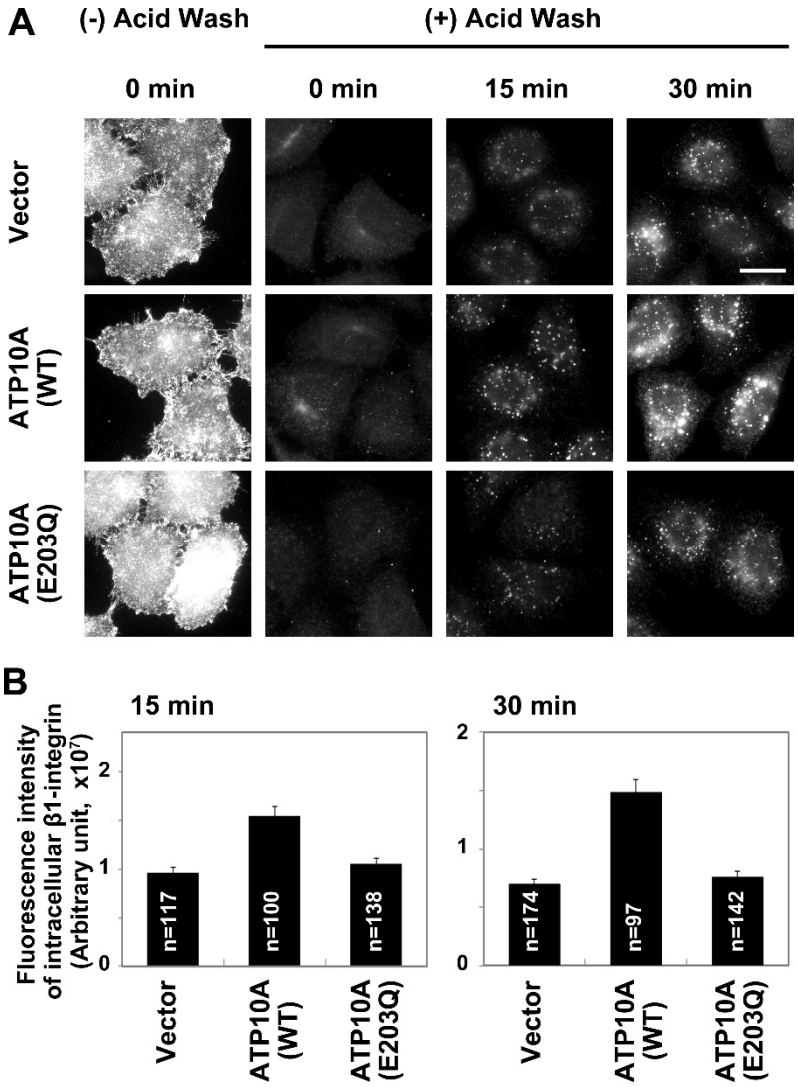

Fig. 2-9. Enhanced PC flipping activity promotes endocytosis of β1-integrin.

HeLa cells stably expressing ATP10A(WT)-HA or ATP10A(E203Q)-HA were incubated with anti-β1-integrin antibody at 4°C for 1 h, washed with PBS to remove unbound antibodies and incubated at 37°C for the indicated times to allow the internalization of β1-integrin. Before fixation, cells were washed with acidic solution to remove the residual antibodies on the plasma membrane. Fixed cells were permeabilized and stained with Cy3-conjugated anti-rat and Alexa Fluor 488-conjugated anti-mouse antibodies (*A*). *Bar*, 20 μm. *B*, Fluorescence intensities of the internalized β1-integrin were quantitated using the MetaMorph software. Graphs show averages ± S.E. from more than 97 cells.

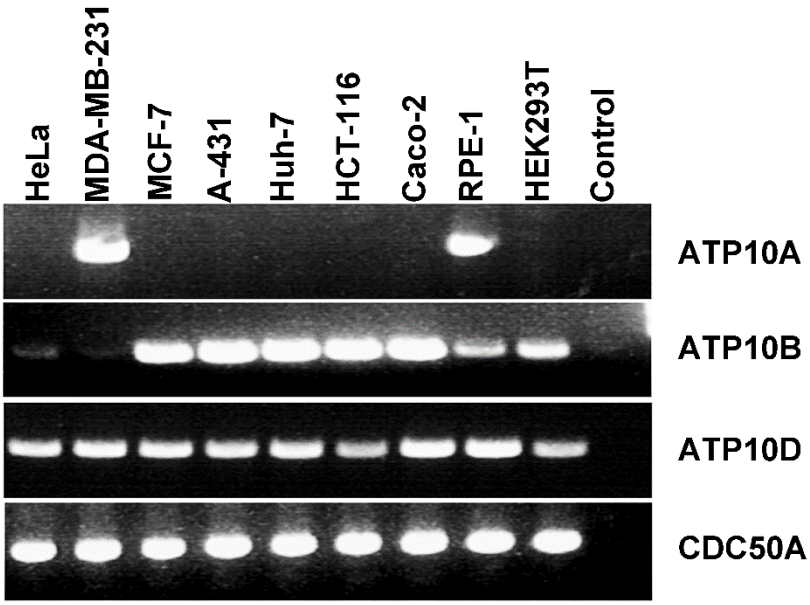

Fig. 2-10. RT-PCR analysis for ATP10 family mRNA in various cell lines.

RT-PCR was performed using total RNA isolated from the indicated cell lines. In control reaction, template RNA was not added. Primers are shown in Table 1.

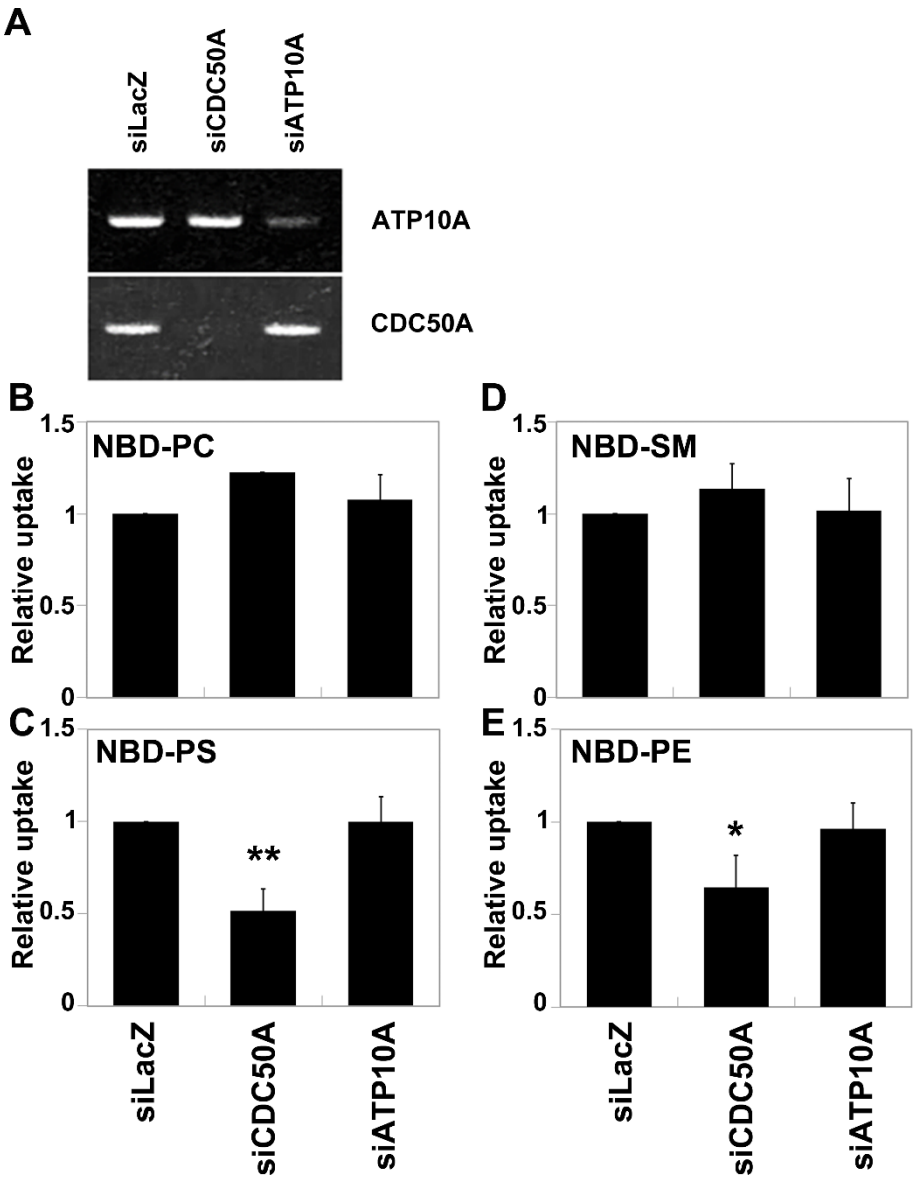

Fig. 2-11. Depletion of CDC50A or ATP10A does not affect basal PC flipping activity in MDA-MB-231 cells.

MDA-MB-231 cells were treated with a pool of siRNA for LacZ, CDC50A, or ATP10A for 120 h. *A*, Cells were lysed to isolate total RNA, which were processed for RT-PCR. *B*, Cells were incubated with the indicated NBD-lipids at 15°C, and the residual fluorescence intensity associated with the cells was determined by flow cytometry as described in the legend for Fig. 2-2. The fold increase in NBD-lipid uptake compared with siLacZ-treated control cells is shown. Graphs display averages ± S.D. from three independent experiments (*, $p<0.05$, **, $p<0.01$).

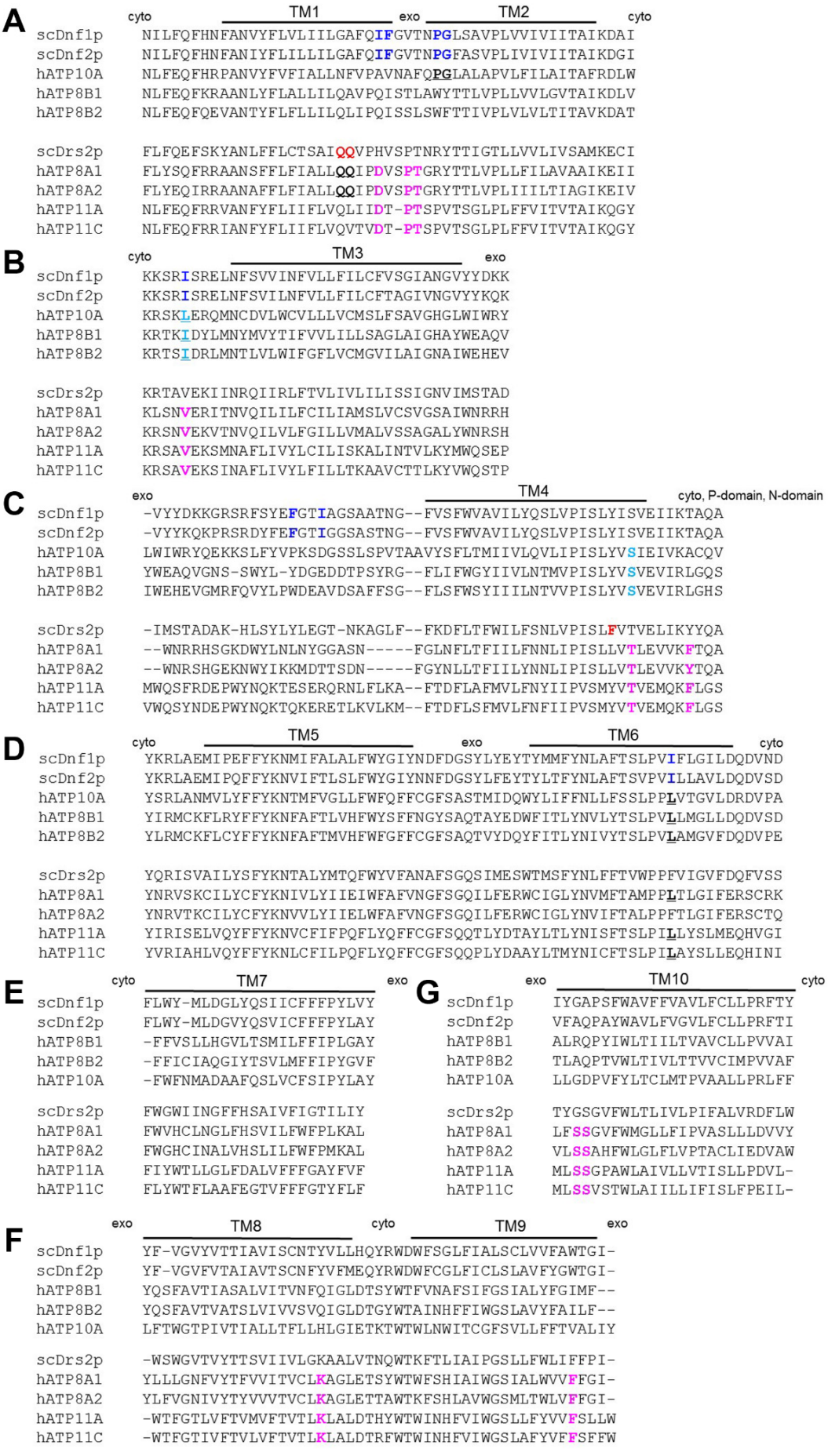
A
cyto
TM1
exo
TM2
cyto
scDnf1p NILFQFHNFANVYFLVLIILGAFQIFGVTNPGLSAVPLVVIVIITAIKDAI
scDnf2p NILFQFHNFANIYFLILLILGAFQIFGVTNPGFASVPLIVIVIITAIKDGI
hATP10A NLFEQFHRPANVYFVFIALLNFVPAVNAFQPGLALAPVLFILAITAFRDLW
hATP8B1 NLFEQFKRAANLYFLALLILQAVPQISTLAWYTTLVPLLVVLGVTAIKDLV
hATP8B2 NLFEQFQEVANTYFLFLLILQLIPQISSLSWFTTIVPLVLVLTITAVKDAT
scDrs2p FLFQEFSKYANLFFLCTSAIQQVPHVSPTNRYTTIGTLLVVLIVSAMKECI
hATP8A1 FLYSQFRRAANSFFLFIALLQQIPDVSPTGRYTTLVPLLFILAVAAIKEII
hATP8A2 FLYEQIRRAANAFFLFIALLQQIPDVSPTGRYTTLVPLIIILTIAGIKEIV
hATP11A NLFEQFRRVANFYFLIIFLVQLIIDT-PTSPVTSGLPLFFVITVTAIKQGY
hATP11C NLFEQFRRIANFYFLIIFLVQVTVDT-PTSPVTSGLPLFFVITVTAIKQGY
B
cyto
TM3
exo
scDnf1p KKSRISRELNFSVVINFVLLFILCFVSGIANGVYYDKK
scDnf2p KKSRISRELNFSVILNFVLLFILCFTAGIVNGVYYKQK
hATP10A KRSKLERQMNCDVLWCVLLLVCMSLFSAVGHGLWIWRY
hATP8B1 KRTKIDYLMNYMVYTIFVVLILLSAGLAIGHAYWEAQV
hATP8B2 KRTSIDRLMNTLVLWIFGFLVCMGVILAIGNAIWEHEV
scDrs2p KRTAVEKIINRQIIRLFTVLIVLILISSIGNVIMSTAD
hATP8A1 KLSNVERITNVQILILFCILIAMSLVCSVGSAIWNRRH
hATP8A2 KRSNVEKVTNVQILVLFGILLVMALVSSAGALYWNRSH
hATP11A KRSAVEKSMNAFLIVYLCILISKALINTVLKYMWQSEP
hATP11C KRSAVEKSINAFLIVYLFILLTKAAVCTTLKYVWQSTP
C
exo
TM4
cyto, P-domain, N-domain
scDnf1p -VYYDKKGRSRFSYEFGTIAGSAATNG--FVSFWVAVILYQSLVPISLYISVEIIKTAQA
scDnf2p -VYYKQKPRSRDYFEFGTIGGSASTNG--FVSFWVAVILYQSLVPISLYISVEIIKTAQA
hATP10A LWIWRYQEKKSLFYVPKSDGSSLSPVTAAVYSFLTMIIVLQVLIPISLYVSIEIVKACQV
hATP8B1 YWEAQVGNS-SWYL-YDGEDDTPSYRG--FLIFWGYIIVLNTMVPISLYVSVEVIRLGQS
hATP8B2 IWEHEVGMRFQVYLPWDEAVDSAFFSG--FLSFWSYIIILNTVVPISLYVSVEVIRLGHS
scDrs2p -IMSTADAK-HLSYLYLEGT-NKAGLF--FKDFLTFWILFSNLVPISLFVTVELIKYYQA
hATP8A1 --WNRRHSGKDWYLNLNYGGASN-----FGLNFLTFIILFNNLIPISLLVTLEVVKFTQA
hATP8A2 --WNRSHGEKNWYIKKMDTTSDN-----FGYNLLTFIILYNNLIPISLLVTLEVVKYTQA
hATP11A MWQSFRDEPWYNQKTESERQRNLFLKA--FTDFLAFMVLFNYIIPVSMYVTVEMQKFLGS
hATP11C VWQSYNDEPWYNQKTQKERETLKVLKM--FTDFLSFMVLFNFIIPVSMYVTVEMQKFLGS
D
cyto
TM5
exo
TM6
cyto
scDnf1p YKRLAEMIPEFFYKNMIFALALFWYGIYNDFDGSYLYEYTYMMFYNLAFTSLPVIFLGILDQDVND
scDnf2p YKRLAEMIPQFFYKNVIFTLSLFWYGIYNNFDGSYLFEYTYLTFYNLAFTSVPVILLAVLDQDVSD
hATP10A YSRLANMVLYFFYKNTMFVGLLFWFQFFCGFSASTMIDQWYLIFFNLLFSSLPPLVTGVLDRDVPA
hATP8B1 YIRMCKFLRYFFYKNFAFTLVHFWYSFFNGYSAQTAYEDWFITLYNVLYTSLPVLLMGLLDQDVSD
hATP8B2 YLRMCKFLCYFFYKNFAFTMVHFWFGFFCGFSAQTVYDQYFITLYNIVYTSLPVLAMGVFDQDVPE
scDrs2p YQRISVAILYSFYKNTALYMTQFWYVFANAFSGQSIMESWTMSFYNLFFTVWPPFVIGVFDQFVSS
hATP8A1 YNRVSKCILYCFYKNIVLYIIEIWFAFVNGFSGQILFERWCIGLYNVMFTAMPPLTLGIFERSCRK
hATP8A2 YNRVTKCILYCFYKNVVLYIIELWFAFVNGFSGQILFERWCIGLYNVIFTALPPFTLGIFERSCTQ
hATP11A YIRISELVQYFFYKNVCFIFPQFLYQFFCGFSQQTLYDTAYLTLYNISFTSLPILLYSLMEQHVGI
hATP11C YVRIAHLVQYFFYKNLCFILPQFLYQFFCGFSQQPLYDAAYLTMYNICFTSLPILAYSLLEQHINI
E
cyto
TM7
exo
scDnf1p FLWY-MLDGLYQSIICFFFPYLVY
scDnf2p FLWY-MLDGVYQSVICFFFPYLAY
hATP8B1 -FFVSLLHGVLTSMILFFIPLGAY
hATP8B2 -FFICIAQGIYTSVLMFFIPYGVF
hATP10A -FWFNMADAAFQSLVCFSIPYLAY
scDrs2p FWGWIINGFFHSAIVFIGTILIY
hATP8A1 FWVHCLNGLFHSVILFWFPLKAL
hATP8A2 FWGHCINALVHSLILFWFPMKAL
hATP11A FIYWTLLGLFDALVFFFGAYFVF
hATP11C FLYWTFLAAFEGTVFFFGTYFLF
G
exo
TM10
cyto
scDnf1p IYGAPSFWAVFFVAVLFCLLPRFTY
scDnf2p VFAQPAYWAVLFVGVLFCLLPRFTI
hATP8B1 ALRQPYIWLTIILTVAVCLLPVVAI
hATP8B2 TLAQPTVWLTIVLTTVVCIMPVVAF
hATP10A LLGDPVFYLTCLMTPVAALLPRLFF
scDrs2p TYGSGVFWLTLIVLPIFALVRDFLW
hATP8A1 LFSSGVFWMGLLFIPVASLLLDVVY
hATP8A2 VLSSAHFWLGLFLVPTACLIEDVAW
hATP11A MLSSGPAWLAIVLLVTISLLPDVL-
hATP11C MLSSVSTWLAIILLIFISLFPEIL-
F
exo
TM8
cyto
TM9
exo
scDnf1p YF-VGVYVTTIAVISCNTYVLLHQYRWDWFSGLFIALSCLVVFAWTGI-
scDnf2p YF-VGVFVTAIAVTSCNFYVFMEQYRWDWFCGLFICLSLAVFYGWTGI-
hATP8B1 YQSFAVTIASALVITVNFQIGLDTSYWTFVNAFSIFGSIALYFGIMF--
hATP8B2 YQSFAVTVATSLVIVVSVQIGLDTGYWTAINHFFIWGSLAVYFAILF--
hATP10A LFTWGTPIVTIALLTFLLHLGIETKTWTWLNWITCGFSVLLFFTVALIY
scDrs2p -WSWGVTVYTTSVIIVLGKAALVTNQWTKFTLIAIPGSLLFWLIFFPI-
hATP8A1 YLLLGNFVYTFVVITVCLKAGLETSYWTWFSHIAIWGSIALWVVFFGI-
hATP8A2 YLFVGNIVYTYVVVTVCLKAGLETTAWTKFSHLAVWGSMLTWLVFFGI-
hATP11A -WTFGTLVFTVMVFTVTLKLALDTHYWTWINHFVIWGSLLFYVVFSLLW
hATP11C -WTFGTIVFTVLVFTVTLKLALDTRFWTWINHFVIWGSLAFYVFFSFFW

Fig. 2-12. Sequence alignment of PC- and PS-flipping P4-ATPases.

The *upper* and *lower panels* show PC- and PS-flipping P4-ATPases, respectively. Bold blue letters and red letters are putative residues for PC- and PS-specificity, respectively, in yeast P4-ATPases (48, 49). Bold light blue letters and bold pink letters represent residues conserved among human PC-flippases and PS-flippases, respectively. TM, transmembrane; exo, exoplasmic; cyto, cytoplasmic; P-domain, phosphorylation domain; N-domain, nucleotide-binding domain

DISCUSSION

In this chapter, I revealed that ATP10A has a PC-specific flippase activity at the plasma membrane (Fig. 2-2). Moreover, the enhanced PC flipping activity resulting from ATP10A expression leads to changes in cell shape, promotes endocytosis of β1-integrin, and delays cell adhesion and spreading.

The PC-flippase activity in cells stably expressing ATP10A was abolished by depletion of CDC50A, confirming that CDC50A is critical for plasma membrane localization of ATP10A (Fig. 2-5). I did not detect any flippase activity of ATP10D toward PC, PS, PE, and SM. ATP10D may have flippase activities toward other lipids that were not tested in this study or may exhibit activity in response to specific signaling events. A genome wide association study from European populations revealed that *ATP10D* variants are associated with accumulation of glucosylceramide in plasma (31), implicating a possibility that ATP10D may exhibit flippase activity toward sphingolipids.

In yeast, Dnf1p prefers PC and PE (11, 47), whereas Drs2p prefers PS (13). Several key residues have been proposed to determine the phospholipid specificities of Drs2p and Dnf1p (48, 49). I aligned and compared the primary sequences between the PS- and PC-flipping P4-ATPases in yeast and human (Fig. 2-12) (21, 39). Many of the key residues required for the PC flipping activity of Dnf1p (*bold blue letters*) or those for the PS flipping activity of Drs2p (*bold red letters*) are not conserved in PC-flipping (ATP10A, ATP8B1, and ATP8B2) or PS-flipping (ATP8A1, ATP8A2, ATP11A, and ATP11C) human P4-ATPases, respectively (Fig. 2-12B). The Ile residue located in the cytoplasmic region close to the transmembrane domain 3 (TM3), is conserved among yeast and human PC-flippases (Fig. 2-12B, *bold light blue letters*), raising a question of whether these residues are critical for determining substrate specificities.

The increase in PC flipping activity resulting from ATP10A expression may alter the plasma membrane dynamics, resulting in drastic changes in cell shape and reduction in cell size (Fig. 2-6). Moreover, cell adhesion and spreading onto the ECM were significantly delayed by ATP10A expression (Figs. 2-7 and 2-8). In addition, expression of ATP10A promoted the endocytosis of β1-integirn (Fig. 2-9). Whereas, expression of ATP10A(E203Q), an ATPase-deficient mutant, did not give rise to any

phenotype observed in ATP10A expression, indicating that these phenotypic changes are ascribed to the PC flippase activity at the plasma membrane. Since ATP10A is expressed in highly invasive and motile cells (Fig. 2-10), it raises the possibility that ATP10A may participate in cell migration and invasion through its PC-flippase activity. Although the exact molecular mechanism underlying the phenotypic changes induced by ATP10A expression remains to be addressed in future studies, I propose two hypotheses: 1) Because PC is the most abundant phospholipid in cellular membranes, enhanced translocation of PC from the extracellular to the cytoplasmic leaflet increases the PC ratio of the cytoplasmic leaflet to the extracellular leaflet, favoring positive curvature toward the cytoplasm. The fact that ATP10A expression increased the rate of β1-integrin endocytosis suggests that enhanced PC-flipping activity generates positive membrane curvature toward the cytoplasm and promotes endocytic vesicle formation. Therefore, outward growth of cells, such as cell spreading, might be inhibited, resulting in a reduction in cell size. In support of this, all of yeast and some of human P4-ATPases are involved in membrane trafficking (38, 39, 41). 2) The enhanced translocation of PC to the cytoplasmic leaflet may reduce the local concentration of PS or phosphatidylinositol 4,5-bisphosphate (PIP_2) in the cytoplasmic leaflet. Because PS and PIP_2 play critical roles in remodeling of the actin cytoskeleton for cell adhesion, spreading, and migration, a decrease in the local concentration of PS or PIP_2 might inhibit cell adhesion and spreading. Indeed, in budding yeast, a local concentration of PS is indispensable for recruitment of Cdc42 to polarized bud tips, and both PS concentration and Cdc42 recycling are regulated by the flippase activity of Dnf1p/Dnf2p, which flips PE and PC (50, 51). In support of this, recent study in our laboratory revealed that sequestration of PS in the cytoplasmic leaflet of the plasma membrane by exogenous expression of a PS-specific probe indeed inhibits cell spreading and formation of focal adhesion (52).

Genetic studies demonstrate that Dnf1p/Dnf2p translocate lyso-PE and lyso-PC into the inner/cytoplasmic leaflet of the plasma membrane, and they are in turn converted to PE and PC, respectively, by an acyltransferase. Therefore, lyso-PE and lyso-PC might be sources for the synthesis of PE and PC to support the lipid content and membrane biogenesis in yeast (53). Hence, I cannot exclude the possibility that ATP10A might be able to translocate lyso-PC.

Depletion of CDC50A dramatically decreased an intrinsic PS flipping activity but did not significantly decrease a PC flipping activity in HeLa and MDA-MB-231 cells. In addition, depletion of ATP10A in MDA-MB-231 cells did not affect the intrinsic PC-flipping activity as well. Therefore, it is likely that the basal PC flipping activity by endogenous P4-ATPases is not as high as the PS flipping activity, which is indispensable for preventing unnecessary exposure of PS on the cell surface. On the other hand, knock-out of CDC50A in KBM-7 cells dramatically decreases flipping activity toward PC as well as PS (27) (data not shown). In addition, the PC flipping activity of ATP8B1 is required for proper bile excretion in the liver (21, 23, 54). Therefore, the level of intrinsic PC flipping activity might vary in different cell types and tissues, raising questions about the regulation of PC flippase activity. In budding yeast, the P4-ATPases (preferentially Dnf1p and Dnf2p) require phosphorylation by Fpk1 for their functions (55), and Drs2p requires an interaction with phosphatidylinositol 4-phosphate for its activity (56). In mammals, PS flipping activity of ATP8A2 is regulated by phosphorylation of a serine residue within a CaMKII targeting motif in its C-terminal cytoplasmic region (58). Moreover, the ATPase activities of ATP11A and ATP11C were inhibited in the presence of high concentration of Ca^{2+} (57). Therefore, it is tempting to speculate that PC-flipping P4-ATPases might be regulated by phosphorylation in response to specific cellular signaling events or by their interactions with specific regulatory factors.

CONCLUSIONS

The summary of the results presented in this study is as follows:

Chapter 1

1. All class 5 P4-ATPases (ATP10A, ATP10B, and ATP10D) interact with CDC50A and require CDC50A for their exit from the ER.
2. ATP10A and ATP10D are localized to the plasma membrane, whereas ATP10B to late endosomes and lysosomes.
3. All class 5 P4-ATPases contain subcellular localization signals in their N-terminal cytoplasmic region.

These results indicate that class 5 P4-ATPases are transported and localized to their final destinations by interaction with CDC50A and participation of localization signals in their N-terminus.

Chapter 2

1. ATP10A is a PC-specific flippase at the plasma membrane.
2. Enhanced PC flipping activity resulting from ATP10A expression alters cell morphology, delays cell adhesion and spreading, and promotes endocytosis of β1-integrin.
3. ATP10A is expressed in limited cell lines possessing high invasive and migratory abilities.

These results suggest that the enhanced PC flipping activity by ATP10A expression alters the transbilayer lipid balance and dynamics of the plasma membrane.

The present study provides new points of view to understand the regulation of the transbilayer lipid distribution not only by classical aminophospholipid translocases but also by PC flippases, and will contribute to understanding physiological functions of class 5 P4-ATPases.

MATERIALS AND METHODS

RT-PCR

Total RNA was isolated from cell lines using the RNeasy Mini Kit (Qiagen) or Isogen (Nippon Gene), and was subjected to RT-PCR analysis using the SuperScript III One-Step RT-PCR system (Invitrogen). Sequences of primers are shown in Table.1.

Plasmids

Expression vectors for C-terminally HA-tagged P4-ATPases and N-terminally FLAG-tagged CDC50A or CDC50B were constructed as described previously (59). The ABCB4 cDNA (a kind gift from Kazumitsu Ueda, Kyoto University) was cloned into the pENTR3C vector (Invitrogen). The pCAG expression vector with C-terminal HA tag was prepared as described previously (59). Transfer of the ABCB4 cDNA to the pCAG-HA expression vectors was performed using the Gateway system (Invitrogen). Chimeric ATP10 mutants with N-terminal replacement were constructed using SLiCE cloning method (60); ATP10BA, N-terminal 1-93 amino acids (a.a.) from ATP10B fused to 87-1499 a.a. of ATP10A; ATP10AB, N-terminal 1-77 a.a. from ATP10A fused to 85-1462 a.a. of ATP10B; ATP10DB, N-terminal s 1-89 a.a. from ATP10D fused to 85-1462 a.a. of ATP10B.

Antibodies and Reagents

The sources of antibodies used in the present study were as follows: monoclonal mouse TfnR (H68.4) was from Zymed Laboratories Inc.; monoclonal mouse anti-calnexin, anti-EEA1, and anti-Lamp-1 and monoclonal rat anti-β1-integrin (Mab13) from BD Biosciences; monoclonal rat anti-HA (3F10) from Roche Applied Science; polyclonal rabbit anti-FLAG from Sigma-Aldrich; monoclonal mouse anti-DYKDDDK (1E6) from Wako Pure Chemical Industries; mouse anti-β-tubulin from Millipore; monoclonal rabbit anti-ATP1A1 from Abcam; Alexa Fluor 488-conjugated monoclonal mouse anti-CD147 (HIM6) from BioLegend; monoclonal mouse anti-MHC-I (W6/32) from ATCC; Alexa Fluor-conjugated secondary antibodies from Molecular Probes; and Cy3-conjugated, Dylight649-conjugated, and horseradish

peroxidase-conjugated secondary antibodies from Jackson ImmunoResearch Laboratories. Alexa Fluor 488-conjugated phalloidin was purchased from Molecular Probes, and fibronectin from Sigma. The NBD labeled phospholipids (Avanti Polar Lipids) used were NBD-PS (1-oleoyl-2-[6-[(7-nitro-2–1,3-benzoxadiazol-4-yl)amino]-hexanoyl]-sn-glycero-3-phosphoserine), NBD-PE (1-oleoyl-2-[6-[(7-nitro-2–1,3-benzoxadiazol-4-yl)amino]hexanoyl]-snglycero-3-phosphoethanolamine), NBD-PC (1-oleoyl-2-[6-[(7-nitro-2–1,3-benzoxadiazol-4-yl)amino]hexanoyl]-sn-glycero-3-phosphocholine), and NBD-SM (N-[6-[(7-nitro-2–1,3-benzoxadiazol-4-yl)amino]hexanoyl]-sphingosine-1-phosphocholine).

Cell Culture, siRNA-mediated Knockdown, and Immunofluorescence Analysis

HeLa cells were maintained in Eagle's minimum essential medium (Nacalai Tesque, Inc.) supplemented with 5 or 10% heat-inactivated FBS (Invitrogen) and non-essential amino acids (Nacalai Tesque). MDA-MB-231 cells were maintained in Dulbecco's modified Eagle's medium containing 4.5 g/l glucose (Nacalai Tesque) supplemented with 10% heat-inactivated FBS. Preparation of pools of siRNAs for CDC50A and ATP10A and knockdown using these siRNA pools were performed as described previously (20, 59). Briefly, a pool of siRNAs directed against nucleotides 597–1086 of CDC50A mRNA or nucleotides 655–1399 of ATP10A mRNA (the A residue of the initiation Met codon was defined as nucleotide 1) was prepared using the BLOCK-iT RNAi TOPO transcription kit and BLOCK-iT Dicer RNAi kit (Invitrogen) or the Replicator RNAi kit and PowerCut Dicer^{TM} (Finnzymes). Cells were transfected with the siRNA pool using Lipofectamine 2000 (Invitrogen) and incubated for 24 h. The transfected cells were then transferred to a culture dish containing coverslips, incubated for an additional 48 h, and processed for immunoblotting, immunofluorescence, and RT-PCR analyses. For retroviral production, pMXs-neo-derived vectors for expression of HA-tagged P4-ATPases were co-transfected with pEF-gag-pol and pCMV-VSVG-Rsv-Rev into HEK293T cells as described previously (20). The pMXs vector and the pEF-gag-pol plasmid were kind gifts from Toshio Kitamura (The University of Tokyo) and the pCMV-VSVG-Rsv-Rev plasmid was kind gift from

Hiroyuki Miyoshi (RIKEN BioResource Center). The resultant retroviruses were concentrated and then used to infect HeLa cells to establish stable cell lines. The infected cells were selected in medium containing G418 (1 mg/ml). To transiently express P4-ATPases, HeLa cells were transfected with a pCAG-HA-based vector carrying P4-ATPase cDNA and a pcDNA3-FLAG-based vector carrying CDC50A cDNA (20) using X-tremeGENE 9 (Roche Applied Science) or Polyethylenimine Max (Polysciences). Two days later, the transfected cells were fixed for immunofluorescence or lysed for immunoblotting analysis. Immunofluorescence staining was performed as described previously (61, 62) and observed using an Axiovert 200MAT microscope (Carl Zeiss, Thornwood, NY). For the plasma membrane staining, cells were incubated with Alexa Fluor 488-conjugated anti-CD147 or anti-MHC-I antibody for 10 min at room temperature prior to fixation. The fixed cells were permeabilized and processed for immunofluorescence analysis. To obtain quantitative data of cellular areas, the surface areas of cells were stained with anti-MHC-I antibody, and CDC50A- or P4-ATPase-expressing cells were chosen. The areas of the cells were measured with the ImageJ software.

Flippase Assay

Incorporation of NBD-phospholipids was analyzed by flow cytometry as described previously (21). Cells were detached from dishes in PBS containing 5 mM EDTA and then harvested by centrifugation. The cells (1×10^6 cells/sample) were washed and equilibrated at 15°C for 15 min in 500 µl of Hanks' balanced salt solution (pH 7.4) containing 1 g/liter glucose (HBSS-glucose). An equal volume of 2 µM NBD-phospholipid in HBSS-glucose was added to the cell suspension and incubated at 15°C. At each time point, 200 µl of cell suspension was collected and mixed with 200 µl of ice-cold HBSS-glucose containing 5% fatty acid-free BSA (Wako Pure Chemical Industries) in order to extract NBD-lipids incorporated into the exoplasmic leaflet of the plasma membrane, as well as unincorporated ones. Next, 5,000 or 10,000 cells were analyzed with a FACSCalibur flow cytometer (BD Biosciences) to measure fluorescence of NBD-lipids translocated into the cytoplasmic leaflet of the plasma membrane, and the mean fluorescence intensity per cell was calculated. Propidium iodide-positive cells (i.e. dead cells) were excluded from the analysis. A one-way

ANOVA was performed to assess variance and comparisons made with Tukey's post hoc analysis.

Immunoprecipitation

HeLa cells were transfected using polyethyleneimine with different combinations of expression vectors for P4-ATPase and CDC50, and grown for 2 days. The cells were then lysed in lysis buffer (20 mM HEPES (pH 7.4), 150 mM NaCl, 1 mM EDTA, and 1% Nonidet P-40) containing a protease inhibitor mixture (Nacalai Tesque) at 4°C for 30 min. The lysates were centrifuged at maximum speed for 20 min at 4°C in a microcentrifuge to remove cellular debris and insoluble materials. The supernatant was incubated with an anti-HA antibody at 4°C for 15 min and then incubated with protein G-coupled Dynabeads (Invitrogen) at 4°C overnight. After washing, the beads were incubated in SDS sample buffer including β-mercaptoethanol at 37°C for 2 h, and the supernatant was subjected to SDS-PAGE and immunoblot analysis using rat anti-HA, mouse anti-DYKDDDK, or mouse anti-β-tubulin antibody. Immunoblots were developed using a Chemi-Lumi One L or Chemi-Lumi One Super kit (Nacalai Tesque), recorded on a LAS-3000 bioimaging system (Fujifilm), and quantified using Image Gauge software (version 4.0, Fujifilm). For cross-linker treatment, 10 mM (dithiobis[succinimidylpropionate]) (DSP, Thermo Scientific) was freshly prepared by dissolving in dimethyl sulfoxide. Transfected cells were washed twice with PBS++ (including 0.1 mM $CaCl_2$ and 0.1 mM $MgCl_2$) and treated with 1 mM DSP in PBS++ for 30 min at room temperature. To stop the reaction, 1 M Tris (pH 7.5) was added at a final concentration of 20 mM and incubated for 15 min at room temperature. The cells were washed with PBS(-), lysed, and immunoprecipitated as described above.

Cell Adhesion and Spreading Assay

HeLa cells were detached from dishes in PBS containing 5 mM EDTA and harvested by centrifugation. The cells were washed and resuspended in complete growth medium, plated onto 24-well plates (1×10^5 cells/well), and incubated at 37°C in 5% CO_2 for the indicated times. The same number of cells was removed, and DNA content was measured using a Qubit fluorometer (Life Technologies). After incubation at 37°C,

the cells were fixed with 96% of ethanol and stained with 1% crystal violet in 10% ethanol at room temperature. After the cells were washed with PBS, the stain was extracted using 1% Triton X-100 and processed to measure absorbance at 570 nm. Absorbance was normalized to the ratio of DNA content. For the cell spreading assay, cells were harvested as described above, washed with serum-free Eagle's minimum essential medium, and seeded onto fibronectin-coated or FBS-coated coverslips. After incubation at 37°C in 5% CO_2 for the indicated times, cells were fixed with 3% paraformaldehyde and subjected to immunofluorescence analysis. Alexa Fluor 488-conjugated phalloidin was added during incubation with secondary antibody. Immunofluorescence staining was performed as described previously (61, 62) and observed using an Axiovert 200 MAT microscope (Carl Zeiss). To obtain quantitative data on the extent of cell spreading, cells were stained with phalloidin, and randomly chosen fields were acquired. Cell areas were measured using MetaMorph software (Molecular Devices)

Integrin Internalization assay

HeLa cells stably expressing ATP10A-HA or ATP10A(E203Q)-HA were incubated with anti-β1-integrin antibody (Mab13) at 4°C for 1 h. Cells were washed with ice-cold PBS, and incubated in medium without the antibody at 37°C for the indicated times. Before fixation, cells were washed with acidic solution (0.5% acetic acid and 0.5 M NaCl, pH 3.0) to remove the residual antibodies on the plasma membrane. Cells were fixed, processed for immunofluorescence analysis, and observed using an Axiovert 200 MAT microscope. The fluorescence intensity of intracellularβ1-integrin was quantitated using the MetaMorph software.

Table 1. Primer sequences used for RT-PCR.

Gene	Forward	Reverse
ATP10A	5'- cacaatgttcgtgggcctcc -3'	5'- cacaatgttcgtgggcctcc -3'
ATP10B	5'- caggatccagcaactatgagaag -3'	5'- ggacaccatgacagatgggcag -3'
ATP10D	5'- ccgagccacaccgctgcag -3'	5'- cagtaatcagtcatggatgttcc -3'
CDC50A	5'- gaaaaagaaaggtattgcttggtg -3'	5'- gtaatgtcagctgtattactactg -3‘

ACKNOWLEDGEMENTS

I would like to thank Professor Kazuhisa Nakayama for his valuable suggestions and helpful discussion. I would also express my special thanks to Associate Professor Hye-Won Shin for her superior guidance and suggestions through this work.

I would like to thank Dr. Hiroyuki Takatsu, Ms. Rie Miyano, Mr. Naoto Takada, and Ms. Sayuri Okamoto for technical supports and helpful discussion.

I would like to express my appreciation Dr. Eri Segi-Nishida, Dr. Yohei Katoh, Dr. Senye Takahashi, Dr. Zhiqiu Man, Dr. Kouhei Takashima, Dr. Yuki Imoto, Ms. Keiko Baba, Ms. Waka Nakai, Mr. Takahiro Shima, Mr. Hiroyuki Umino, Ms. Natsuki Ono, Mr. Teruki Funabashi, Mr. Yohei Hagiya, Mr. Shohei Nozaki, Mr. Gaku Tanaka, Mr. Yoshiki Tanaka, Mr. Takashi Matsumoto, and Mr. Masahiro Takayama for their technical advice and helpful discussion.

I also thank members of the Department of Physiological Chemistry, Graduate School of Pharmaceutical Sciences, Kyoto University for their continuous encouragements, helpful discussions and technical supports.

I would like to thank my family for persistent understanding and support for many things.

I was supported by Grant-in-Aid for JSPS research fellow.

REFERENCES

1. Op den Kamp, J. A. (1979) Lipid asymmetry in membranes. *Annual Rev. Biochem.* **48**, 47-71
2. van Meer, G., Voelker, D. R., and Feigenson, G. W. (2008) Membrane lipids: where they are and how they behave. *Nat. Rev. Mol. Cell Biol.* **9**, 112-124
3. Leventis, P. A., and Grinstein, S. (2010) The distribution and function of phosphatidylserine in cellular membranes. *Annu. Rev Biophys.* **39**, 407-427
4. Schrier, S. L., Zachowski, A., and Devaux, P. F. (1992) Mechanisms of amphipath-induced stomatocytosis in human erythrocytes. *Blood* **79**, 782-786
5. Zwaal, R. F., and Schroit, A. J. (1997) Pathophysiologic implications of membrane phospholipid asymmetry in blood cells. *Blood* **89**, 1121-1132
6. van den Eijnde, S. M., van den Hoff, M. J., Reutelingsperger, C. P., van Heerde, W. L., Henfling, M. E., Vermeij-Keers, C., Schutte, B., Borgers, M., and Ramaekers, F. C. (2001) Transient expression of phosphatidylserine at cell-cell contact areas is required for myotube formation. *J. Cell Sci*. **114**, 3631–3642
7. Williamson, P., and Schlegel, R. A. (2002) Transbilayer phospholipid movement and the clearance of apoptotic cells. *Biochim. Biophys. Acta* **1585**, 53–63
8. Seigneuret, M., and Devaux, P. F. (1984) ATP-dependent asymmetric distribution of spin labeled phospholipids in the erythrocyte membrane: relation to shape changes. *Proc. Natl. Acad. Sci. USA* **81**, 3751-3755
9. Tang, X., Halleck, M. S., Schlegel, R. A., and Williamson, P. (1996) A subfamily of P-type ATPases with aminophospholipid transporting activity. *Science* **272**, 1495-1497
10. Daleke, D. L. (2003) Regulation of transbilayer plasma membrane phospholipid asymmetry. *J. Lipid Res.* **44**, 233-242
11. Pomorski, T., Lombardi, R., Riezman, H., Devaux, P. F., van Meer, G., and Holthuis, J. C. M. (2003) Drs2p-related P-type ATPases Dnf1p and Dnf2p Are Required for Phospholipid Translocation across the Yeast Plasma Membrane and Serve a Role in Endocytosis. *Mol. Biol. Cell* **14**, 1240-1254
12. Saito, K., Fujimura-Kamada, K., Furuta, N., Kato, U., Umeda, M., and Tanaka, K. (2004) Cdc50p, a Protein Required for Polarized Growth, Associates with the

Drs2p P-Type ATPase Implicated in Phospholipid Translocation in Saccharomyces cerevisiae. *Mol. Biol. Cell* **15**, 3418-3432

13. Zhou, X., and Graham, T. R. (2009) Reconstitution of phospholipid translocase activity with purified Drs2p, a type-IV P-type ATPase from budding yeast. *Proc. Natl. Acad. Sci. USA* **106**, 16586-16591
14. Kühlbrandt, W. (2004) Biology, structure and mechanism of P-type ATPases. *Nat. Rev. Mol. Cell Biol.* **5**, 282–295
15. Furuta, N., Fujimura-Kamada, K., Saito, K., Yamamoto, T., and Tanaka, K. (2007) Endocytic Recycling in Yeast Is Regulated by Putative Phospholipid Translocases and the Ypt31p/32p-Rcy1p Pathway. *Mol. Biol. Cell* **18**, 295-312
16. Paulusma, C. C., Folmer, D. E., Ho-Mok, K. S., de Waart, D. R., Hilarius, P. M., Verhoeven, A.J., and Oude Elferink, R. P. (2008) ATP8B1 requires an accessory protein for endoplasmic16reticulum exit and plasma membrane lipid flippase activity. *Hepatology* **47**, 268-278
17. Bryde, S., Hennrich, H., Verhulst, P. M., Devaux, P. F., Lenoir, G., and Holthuis, J. C. (2010) CDC50 Proteins Are Critical Components of the Human Class-1 P4-ATPase Transport Machinery. *J. Biol. Chem.* **285**, 40562-40572
18. van der Velden, L. M., Wichers, C. G. K., van Breevoort, A. E. D., Coleman, J. A., Molday, R.S., Berger, R., Klomp, L. W. J., and van de Graaf, S. F. J. (2010) Heteromeric Interactions Required for Abundance and Subcellular Localization of Human CDC50 Proteins and Class 1 P4-ATPases. *J. Biol. Chem.* **285**, 40088-40096
19. Coleman, J. A., and Molday, R. S. (2011) Critical Role of the b-Subunit CDC50A in the Stable Expression, Assembly, Subcellular Localization, and Lipid Transport Activity of the P4-ATPase ATP8A2. *J. Biol. Chem.* **286**, 17205-17216
20. Takatsu, H., Baba, K., Shima, T., Umino, H., Kato, U., Umeda, M., Nakayama, K., and Shin, H.-W. (2011) ATP9B, a P4-ATPase (a Putative Aminophospholipid Translocase), Localizes to the trans-Golgi Network in a CDC50 Protein-independent Manner. *J. Biol. Chem.* **286**, 38159-38167
21. Takatsu, H., Tanaka, G., Segawa, K., Suzuki, J., Nagata, S., Nakayama, K., and Shin, H.-W. (2014) Phospholipid Flippase Activities and Substrate Specificities of Human Type IV P-type ATPases Localized to the Plasma Membrane. *J. Biol. Chem.* **289**, 33543-33556

22. Paulusma, C. C., Groen, A., Kunne, C., Ho-Mok, K. S., Spijkerboer, A. L., Rudi de Waart, D.,Hoek, F. J., Vreeling, H., Hoeben, K. A., van Marle, J., Pawlikowska, L., Bull, L. N., Hofmann, A. F., Knisely, A. S., and Oude Elferink, R. P. (2006) Atp8b1 deficiency in mice reduces resistance of the canalicular membrane to hydrophobic bile salts and impairs bile salt transport. *Hepatology* **44**, 195-204
23. Folmer, D. E., Elferink, R. P. J. O., and Paulusma, C. C. (2009) P4 ATPases - Lipid flippases and their role in disease. *Biochim. Biophys. Acta* **1791**, 628-635
24. Levano, K., Punia, V., Raghunath, M., Debata, P. R., Curcio, G. M., Mogha, A., Purkayastha, S., McCloskey, D., Fata, J., and Banerjee, P. (2012) Atp8a1 deficiency is associated with phosphatidylserine externalization in hippocampus and delayed hippocampus-dependent learning. *J. Neurochem.* **120**, 302-313
25. Yabas, M., Teh, C. E., Frankenreiter, S., Lal, D., Roots, C. M., Whittle, B., Andrews, D. T., Zhang, Y., Teoh, N. C., Sprent, J., Tze, L. E., Kucharska, E. M., Kofler, J., Farell, G. C., Broer, S., Goodnow, C. C., and Enders, A. (2011) ATP11C is critical for the internalization of phosphatidylserine and differentiation of B lymphocytes. *Nat. Immunol.* **12**, 441-449
26. Yabas, M., Coupland, L. A., Cromer, D., Winterberg, M., Teoh, N. C., D'Rozario, J., Kirk, K., Broer, S., Parish, C. R., and Enders, A. (2014) Mice Deficient in the Putative Phospholipid Flippase ATP11C Exhibit Altered Erythrocyte Shape, Anemia and Reduced Erythrocyte17Lifespan. *J. Biol. Chem.* **289**, 19531-19537
27. Segawa, K., Kurata, S., Yanagihashi, Y., Brummelkamp, T. R., Matsuda, F., and Nagata, S. (2014) Caspase-mediated cleavage of phospholipid flippase for apoptotic phosphatidylserine exposure. *Science* **344**, 1164-1168
28. Dhar, M. S., Sommardahl, C. S., Kirkland, T., Nelson, S., Donnell, R., Johnson, D. K., and Castellani, L. W. (2004) Mice heterozygous for Atp10c, a putative amphipath, represent a novel model of obesity and type 2 diabetes. *J. Nutr.* **134**, 799-805
29. Hurst, S. E., Minkin, S. C., Biggerstaff, J., and Dhar, M. S. (2012) Transient Silencing of a Type IV P-Type ATPase, Atp10c, Results in Decreased Glucose Uptake in C2C12 Myotubes. *J. Nutr. Metabol.* **2012**, 152902
30. Dhar, M. S., Yuan, J. S., Elliott, S. B., and Sommardahl, C. (2006) A type IV P-type ATPase affects insulin-mediated glucose uptake in adipose tissue and

skeletal muscle in mice. *J Nutr. Biochem.* **17**, 811-820

31. Vitart, V., Rudan, I., Hicks, A. A., Pramstaller, P. P., Aulchenko, Y., Franklin, C. S., Liebisch, G., Erdmann, J., Jonasson, I., Zorkoltseva, I. V, Pattaro, C., Hayward, C., Isaacs, A., Hengstenberg, C., Polasek, O., Demirkan, A., Kolcic, I., Schwienbacher, C., Igl, W., Biloglav, Z., Wichmann, H., Schunkert, H., Hastie, N., Oostra, B. A., and Wild, S. H. (2009) Genetic Determinants of Circulating Sphingolipid Concentrations in European Populations. *PLoS Genet.* **10**: e1000672
32. Kengia, J.T., Ko, K. C., Ikeda, S., Hiraishi, A., Mieno-naka, M., Arai, T., Sato, N., and Muramatsu, M. (2013) A gene variant in the Atp10d gene associates with atherosclerotic indices in Japanese elderly population. *Atherosclerosis*. **231**, 158-162
33. Flamant, S., Pescher, P., Lamercer, B., Clément-Ziza, M., Képès, F. Milon, G., Marchal, G. and Besmond, C. (2003) Characterization of a putative type IV aminophospholipid transporter P-type ATPase. *Mamm. Genome* **14**, 21-30
34. Anthonisen, A. N., Clausen, J. D., and Andersen, J. P. (2006) Mutational analysis of the conserved TGES loop of sarcoplasmic reticulum Ca2+-ATPase. *J. Biol. Chem.* **281**, 31572-31582
35. Morita, S. Y., Kobayashi, A., Takanezawa, Y., Kioka, N., Handa, T., Arai, H., Matsuo, M., and Ueda, K. (2007) Bile salt-dependent efflux of cellular phospholipids mediated by ATP binding cassette protein B4. *Hepatology* **46**, 188-199
36. Natarajan, P., Wang, J., Hua, Z., and Graham, T. R. (2004) Drs2p-coupled aminophospholipid translocase activity in yeast Golgi membranes and relationship to in vivo function. *Proc. Natl. Acad. Sci. USA* **101**, 10614-10619
37. Wu, Y., Taker, M., Cuentas-Condori, A., and Graham, T.R., (2016) Neo1 and phosphatidylethanolamine contribute to vacuole membrane fusion in *Saccharomyces cerevisiae. Cell. Logist*. **6**, e1228791
38. Graham, T.R. (2004) Flippases and vesicle-mediated protein transport *Trends Cell Biol.* **14,** 1240-1254
39. Lee, S., Uchida, Y., Wang, J., Matsudaira, T., Nakagawa, T., Kishimoto, T., Mukai, K., Inaba, T., Kobayashi, T., Molday, R. S., Taguchi, T., and Arai, H. (2015) Transport through recycling endosomes requires EHD 1 recruitment by a

phosphatidylserine translocase *EMBO J*. **34**, 669-688.

40. Kato, U., Inadome, H., Yamamoto, M., Emoto, K., Kobayashi, T., and Umeda, M. (2013) Role for phospholipid flippase complex of ATP8A1 and CDC50A proteins in cell migration. *J. Biol. Chem*. **288**, 4922–4934
41. Tanaka, Y., Ono, N., Shima, T., Tanaka, G., Katoh, Y., Nakayama, K., Takatsu, H., and Shin, H.-W. (2016) The phospholipid flippase ATP9A is required for recycling pathway from endosomes to the plasma membrane. *Mol. Biol. Cell* **27,** 3883-3893.
42. Folmer, D. E., van der Mark, V. A., Ho-Mok, K. S., Oude Elferink, R. P. J., and Paulusma, C.C. (2009) Differential effects of progressive familial intrahepatic cholestasis type 1 and benign recurrent intrahepatic cholestasis type 1 mutations on canalicular localization of ATP8B1. *Hepatology* **50**, 1597-1605
43. Hynes, R.O. (2002). Integrins: Bidirectional, allosteric signaling machines. *Cell* **110**, 673–687
44. Paul, N. R., Jacquemet, G., and Caswell, P. T. (2015) Endocytic Trafficking of Integrins in Cell Migration. *Curr. Biol.* **25**, R1092-R1105
45. Yu, Y., Xiao, C., Tan, L., Wang, Q., Li, X., and Feng, Y. (2014) Cancer-associated fibroblasts induce epithelial – mesenchymal transition of breast cancer cells through paracrine TGF-β signalling. *Br. J. Cancer* **110**, 724–732
46. Shafaq-Zadah, M., Gomes-Santos, C. S., Bardin, S., Maiuri, P., Maurin, M., Iranzo, J., Gautreau, A., Lamaze, C., Caswell, P., Goud, B., and Johannes, L. (2015) Persistent cell migration and adhesion rely on retrograde transport of β1 integrin. *Nat. Cell Biol*. **18**, 54–64
47. Kato, U., Emoto, K., Fredriksson, C., Nakamura, H., Ohta, A., Kobayashi, T., Murakami-Murofushi, K., Kobayashi, T., and Umeda, M. (2002) A Novel Membrane Protein, Ros3p, Is Required for Phospholipid Translocation across the Plasma Membrane in Saccharomyces cerevisiae. *J. Biol. Chem.* **277**, 37855-37862
48. Baldridge, R. D., and Graham, T. R. (2013) Two-gate mechanism for phospholipid selection18and transport by type IV P-type ATPases. *Proc. Natl. Acad. Sci. USA* **110**, E358-367
49. Baldridge, R. D., and Graham, T. R. (2012) Identification of residues defining phospholipid flippase substrate specificity of type IV P-type ATPases. *Proc. Natl. Acad. Sci. USA* **109**, E290-E298

50. Fairn, G. D., Hermansson, M., Somerharju, P., and Grinstein, S. (2011) Phosphatidylserine is polarized and required for proper Cdc42 localization and for development of cell polarity. *Nat. Cell Biol.* **13**, 1424-1430
51. Das, A., Slaughter, B. D., Unruh, J. R., Bradford, W. D., Alexander, R., Rubinstein, B., and Li,R. (2012) Flippase-mediated phospholipid asymmetry promotes fast Cdc42 recycling in dynamic maintenance of cell polarity. *Nat. Cell Biol.* **14**, 304-310
52. Miyano, R., Matsumoto, T., Takatsu, H., Nakayama, K., and Shin, H.-W. (2016) Alteration of transbilayer phospholipid compositions is involved in cell adhesion, cell spreading, and focal adhesion formation. *FEBS Lett*. **590**, 2138-2145.
53. Riekhof, W. R., and Voelker, D. R. (2009) The yeast plasma membrane P4-ATPases are majortransporters for lysophospholipids. *Biochim. Biophys. Acta* **1791**, 620-627
54. Klomp, L. W., Vargas, J. C., van Mil, S. W., Pawlikowska, L., Strautnieks, S. S., van Eijk, M.J., Juijn, J. A., Pabon-Pena, C., Smith, L. B., DeYoung, J. A., Byrne, J. A., Gombert, J., van der Brugge, G., Berger, R., Jankowska, I., Pawlowska, J., Villa, E., Knisely, A. S., Thompson, R.J., Freimer, N. B., Houwen, R. H., and Bull, L. N. (2004) Characterization of mutations inATP8B1 associated with hereditary cholestasis. *Hepatology* **40**, 27-38
55. Nakano, K., Yamamoto, T., Kishimoto, T., Noji, T., and Tanaka, K. (2008) Protein kinasesFpk1p and Fpk2p are novel regulators of phospholipid asymmetry. *Mol. Biol. Cell* **19**, 1783-1797
56. Natarajan, P., Liu, K., Patil, D. V., Sciorra, V. A., Jackson, C. L., and Graham, T. R. (2009) Regulation of a Golgi flippase by phosphoinositides and an ArfGEF. *Nat. Cell Biol.* **11**, 1421-1426
57. Segawa, K., Kurata, S., and Nagata, S. (2016) Human Type IV P-type ATPases That Work as Plasma Membrane Phospholipid Flippases and Their Regulation by Caspase and Calcium. *J. Biol. Chem.* **291**, 762–72
58. Chalat, M., Moleschi, K., and Molday, R. S. (2017) C-terminus of the P4-ATPase ATP8A2 Functions in Protein Folding and Regulation of Phospholipid Flippase Activity *Mol. Biol. Cell* **28**, 452-462
59. Yamamoto, H., Koga, H., Katoh, Y., Takahashi, S., Nakayama, K., and Shin, H. -W.

(2010) Functional cross-talk between Rab14 and Rab4 through a dual effector, RUFY1/Rabip4. *Mol. Biol. Cell* **21**, 2746-2755

60. Motohashi, K. (2015). A simple and efficient seamless DNA cloning method using SLiCE from Escherichia coli laboratory strains and its application to SLiP site-directed mutagenesis. *BMC Biotechnol*. **15**, 47.
61. Shin, H.-W., Kobayashi, H., Kitamura, M., Waguri, S., Suganuma, T., Uchiyama, Y., and Nakayama, K. (2005) Roles of ARFRP1 (ADP-ribosylation factor-related protein 1) in post-Golgi membrane trafficking. *J. Cell Sci.* **118**, 4039-4048
62. Shin, H.-W., Morinaga, N., Noda, M., and Nakayama, K. (2004) BIG2, a Guanine Nucleotide Exchange Factor for ADP-Ribosylation Factors: Its Localization to Recycling Endosomes and Implication in the Endosome Integrity. *Mol. Biol. Cell* **15**, 5283-5294